



HAL
open science

Multicriteria evaluation of the AquaCrop crop model in a hilly rainfed Mediterranean agrosystem

Mariem Dhouib, Rim Zitouna-Chebbi, Laurent Prevoit, J. Molénat, Insaf Mekki, Frédéric Jacob

► To cite this version:

Mariem Dhouib, Rim Zitouna-Chebbi, Laurent Prevoit, J. Molénat, Insaf Mekki, et al.. Multicriteria evaluation of the AquaCrop crop model in a hilly rainfed Mediterranean agrosystem. *Agricultural Water Management*, 2022, 273, pp.107912. 10.1016/j.agwat.2022.107912 . hal-03771403

HAL Id: hal-03771403

<https://hal.science/hal-03771403v1>

Submitted on 7 Sep 2022

HAL is a multi-disciplinary open access archive for the deposit and dissemination of scientific research documents, whether they are published or not. The documents may come from teaching and research institutions in France or abroad, or from public or private research centers.

L'archive ouverte pluridisciplinaire **HAL**, est destinée au dépôt et à la diffusion de documents scientifiques de niveau recherche, publiés ou non, émanant des établissements d'enseignement et de recherche français ou étrangers, des laboratoires publics ou privés.

1 **Multicriteria evaluation of the AquaCrop crop model in a hilly rainfed Mediterranean**
2 **agrosystem**

3 M. Dhouib (1), R. Zitouna-Chebbi (2), L. Prévot (3), J. Molénat (3), I. Mekki (2), F. Jacob (4)

4 (1) Institut Agro Montpellier/UMR LISAH, INRAE, IRD, Institut Agro Montpellier, Ag-
5 roParisTech, University of Montpellier, Montpellier, France

6 (2) INRGREF, University of Carthage, Tunis, Tunisia

7 (3) INRAE/UMR LISAH, INRAE, IRD, Institut Agro Montpellier, AgroParisTech, Univer-
8 sity of Montpellier, Montpellier, France

9 (4) IRD/UMR LISAH, INRAE, IRD, Agro Montpellier Institute, AgroParisTech, University
10 of Montpellier, Montpellier, France

11 **Abstract**

12 Exploring crop spatial organizations within landscapes is a promising solution for agroecolog-
13 ical transitions and climate change adaptation in Mediterranean rainfed hilly agrosystems. A
14 prerequisite is to ensure that crop models can simulate a range of agrohydrological processes
15 in such agrosystems. The current study deepened the evaluation of the AquaCrop model by
16 conducting a multicriteria evaluation (canopy cover CC, dry aboveground biomass AGB, ac-
17 tual evapotranspiration ET_a , runoff R, soil water content SWC) for a range of crop and soil
18 combinations, and for contrasted hydroclimatic years in northeastern Tunisia. The data were
19 collected in the Kamech catchment (OMERE Observatory) during nine measurement cam-
20 paigns on predominant soils and crops. AquaCrop simulations were based on field observations
21 and parameters from the literature.

1
2
3
4
5
6
7
8
9
10
11
12
13
14
15
16
17
18
19
20
21
22
23
24
25
26
27
28
29
30
31
32
33
34
35
36
37
38
39
40
41
42
43
44
45
46
47
48
49
50
51
52
53
54
55
56
57
58
59
60
61
62
63
64
65

22 AquaCrop could simulate plant dynamics and water fluxes for contrasted hydroclimatic years,
23 with a slight dependence on soil class and a significant dependence on crop type. Model simu-
24 lations were of moderate quality for CC (R^2 of 0.45, RMSE of 0.24 on average) and of accepta-
25 ble quality for AGB (R^2 of 0.81, RMSE of 0.85 ton ha⁻¹ on average). AquaCrop acceptably
26 simulated water transfer across the soil–plant continuum (R^2 of 0.62, RMSE of 0.77 mm day⁻¹
27 on average for ET_a; R^2 of 0.68, RMSE of 0.75 mm day⁻¹ on average for R; R^2 of 0.86, RMSE
28 of 27.4 mm on average for SWC). The model performances were satisfactory for most cases,
29 with p values larger than 5% for the Student’s t test on linear regressions of validation. Our
30 results were similar to those reported in previous studies over flat terrain, including delayed
31 senescence by model simulations with subsequent overestimation of CC and AGB observa-
32 tions. Additionally, soil cracks likely altered the AquaCrop ability to simulate runoff. Despite
33 these limitations, our results support the application of AquaCrop to evaluate water productiv-
34 ity in hilly agrosystems.

35 **Keywords**

36 AquaCrop model; Rainfed agrosystems; Hilly terrains; Multicriteria evaluation; Mediterranean
37 soils and crops; Soil water balance

38 1. Introduction

39 Mediterranean agriculture is an important sector from economic, social and environmental per-
40 spectives, especially for the southern and eastern Mediterranean countries. It is a significant
41 contributor to gross domestic product (GDP) in these countries; it ensures food security, and it
42 helps reduce rural migration by providing local jobs (Tanyeri-Abur, 2015). Rainfed agriculture
43 covers 80% and 75% of cultivated lands in the world and North Africa, respectively
44 (Bhattacharya, 2019; Wani et al., 2009). It is generally based on family systems, and it has
45 significant room for improvement in water productivity (Ruben and Pender, 2004). In hilly
46 areas, the productivity of rainfed agriculture depends not only on the rainfall regime but also
47 on the spatiotemporal distribution of surface water and sediment flows (Norouzi et al., 2010).
48 Until now, Mediterranean public policies within hilly areas have mainly focused on mobilizing
49 blue water resources for irrigated agriculture through the planning of hydroagricultural infra-
50 structures (e.g., dams, reservoirs) and have focused less on optimizing the use of green water
51 for rainfed agriculture (Nouri et al., 2020).

52 Despite of numerous benefits for Mediterranean hilly areas, rainfed agriculture undergoes sev-
53 eral pressures (Brun et al., 2016), either climate-driven (floods and erosion, heat waves, rainfall
54 shortages) or anthropogenic-driven (population growth, increasing agricultural activities and
55 hydroagricultural infrastructures). From a sustainability perspective, it is important to quanti-
56 tatively manage agricultural water, where some of the numerous solutions to be explored in-
57 volve the spatiotemporal modulation of anthropogenic actions, individually or in combination
58 (IAASTD, 2008). These solutions imply processes (fluxes, storages and transformations) and
59 several components (e.g., root zone, aquifer, vegetation, hydroagricultural infrastructures, ag-
60 ricultural practices) within agrosystems. The exploration of these solutions must account for
61 two key points. First, in situ scientific experiments are not suitable for both large agricultural
62 areas and forecasts in a climate change context, which makes necessary the use of process

63 modelling for numerical simulations (Jones et al., 2017). Second, the water cycle and crop
64 dynamics are strongly linked. Vegetation cover drives the rainfall repartition between runoff
65 and infiltration in relation to fluxes within hydrographic networks towards lakes and reservoirs,
66 to soil water storage and to aquifer refill. The water cycle drives root zone water content and
67 crop water consumption, with consequences on agricultural yields. It is therefore important to
68 properly characterize the interactions between the water cycle and crop functioning within ag-
69 rosystems (Kanda et al., 2018).

70 Integrated process modelling should be able to simulate, within hilly catchments, crop func-
71 tioning and the water cycle along with their interactions. This requires parsimonious crop mod-
72 els that (1) minimize the number of parameters for realistic simulations with spatialization pur-
73 poses and (2) simulate crop functioning in relation to water dynamics within the root zone layer
74 and underlying shallow aquifer. The literature provides a large number of crop models that
75 describe plant functioning and growth along with crop yield (Weiss et al., 2020). Well known
76 examples are APSIM (Keating et al., 2003), DSSAT (Jones et al., 2003), EPIC (Williams et
77 al., 1984), STICS (Brisson et al., 2003), WOFOST (Todorovic et al., 2009; de Wit et al., 2019),
78 AquaCrop (Raes et al., 2009; Steduto et al., 2009), CropSyst (Stöckle et al., 2003), or AqYield
79 (Constantin et al., 2015; Tribouillois et al., 2018). Based on the primary factors that describe
80 crop functioning, Todorovic et al. (2009) classified crop models into (1) carbon-driven models
81 such as WOFOST, CROPGRO, and DSSAT, (2) solar radiation-driven models such as
82 CERES, EPIC, STICS, and APSIM, and (3) water-driven models such as AquaCrop and
83 CropSyst in which biomass production is proportional to the amount of transpired water.
84 CropSyst is a model based on water and solar radiation. When the vapour pressure deficit
85 (VPD) is very low, the transpiration-biomass relationship is replaced by a radiative approach
86 in which biomass is determined on the basis of intercepted photosynthetically active radiation

87 (IPAR, Stöckle et al., 2003; Kanda et al., 2018). Among the aforementioned crop models, AquaCrop is therefore the unique water-driven model (Kanda et al., 2018). It is thus an interesting model for addressing the coupling of crop functioning and the water cycle within Mediterranean hilly catchments typified by rainfed agriculture. In addition, it provides a trade-off between robustness and simplicity, since it requires a moderate number of input parameters.

88 The literature includes numerous studies that involve AquaCrop. These studies can be classified into four main groups, according to their content: (1) calibration, validation, and performance evaluation of the model in specific contexts (Mkhabela and Bullock, 2012; Zeleke, 2019); (2) cropping system management on the basis of model simulations: estimation of crop water requirements, sowing dates and crop yields, as well as consequences of fertilization, salinity, and irrigation regimes on crop yield (Araya et al., 2010; Qin et al., 2013; Nyakudya and Stroosnijder, 2014; El Mokh et al., 2017; Er-Raki et al., 2021); (3) impact of climate change on crop production and evaluation of different adaptation strategies (Muluneh, 2020; Raoufi and Soufizadeh, 2020; Rashid et al., 2019); and (4) economic impact of cropping practices and climate change on productivity (Cusicanqui et al., 2013; Bird et al., 2016). Meanwhile, AquaCrop has been used across the five continents, under different climates (Mediterranean, tropical, continental, temperate) and within both irrigated and rainfed agrosystems (Geerts et al., 2009; García-Vila and Fereres, 2012; García-López et al., 2014; Vanuytrecht et al., 2014; Ahmadi et al., 2015; Deb et al., 2015; Shrestha et al., 2016; Silvestro et al., 2017; Xing et al., 2017; Sandhu and Irmak, 2019; Lu et al., 2021). Overall, AquaCrop has been tested and validated on a wide range of agroenvironmental conditions.

89 Some of the aforementioned AquaCrop-based studies focused on variables describing crop growth, such as canopy cover CC, dry aboveground biomass AGB and yield (Todorovic et al., 2009; Mkhabela and Bullock, 2012; Silvestro et al., 2017). Other studies addressed actual evapotranspiration (ET_a) (Geerts et al., 2009; Katerji et al., 2013) as well as soil water content

112 (SWC) (Nyakudya and Stroosnijder, 2014; Sghaier et al., 2014). Similar to most crop models,
113 AquaCrop was designed and evaluated for local applications at the plot level over flat terrains.
114 More recently, the model was evaluated on hilly terrains, either in a multilocal way that disre-
115 garded interplot water exchanges (Alaya et al., 2019; Han et al., 2019) or in a distributed way
116 that accounted for interplot water exchanges (Van Loo and Verstraeten, 2021). However, more
117 research is needed to address the diversity of situations induced by Mediterranean rainfed hilly
118 agrosystems in relation to cropping, soil and topographic conditions. In addition, AquaCrop
119 was evaluated on only a few variables simultaneously, whereas any multicriteria evaluation is
120 likely to provide a better assessment of model capacities.

121 The objective of this study is to deepen the evaluation of the capabilities of the AquaCrop
122 model for rainfed crops within hilly Mediterranean catchments. We propose (1) to consider
123 little-studied crops (e.g., faba bean and oats) under subhumid to semiarid climates, (2) to con-
124 sider combinations of crops (faba bean, oats, wheat, barley) and soils (Vertisols, Cambisols
125 and Luvisols) for contrasted hydroclimatic years, and (3) to conduct a more substantial mul-
126 ticriteria analysis that includes simultaneously vegetation canopy (CC, AGB), soil water con-
127 tent integrated over topsoil and root zones, and water fluxes (ET_a , runoff as infiltration excess).
128 We focus here on the evaluation of AquaCrop without addressing calibration issues. The cur-
129 rent paper is structured as follows. We briefly present the AquaCrop model. We introduce the
130 study area and the datasets used, as well as the strategy for evaluating the model. Thereafter,
131 we analyse the comparison of the simulations against the observations by exploring the possible
132 influences of soil and crop type. We finally discuss these results in light of former studies, and
133 we conclude with our contribution to the assessment of AquaCrop performances, along with
134 further perspectives.

135 2. Presentation of the AquaCrop model

1
2
3 136 Detailed presentations of AquaCrop (<https://www.fao.org/aquacrop/en/>) are given by Steduto
4
5 137 et al., (2009), Raes et al. (2009) and Salman et al. (2021). We detail here the specificities related
6
7
8 138 to the methodological choices on which the current study relies. Developed by FAO, AquaCrop
9
10 139 is a parsimonious (reduced number of parameters) crop model that aims to simulate crop bio-
11
12 140 mass and yield by considering water as the main driver of crop functioning (Kanda et al., 2018).
13
14
15 141 Operating at a daily time step, AquaCrop simulates the vertical exchanges between the different
16
17 142 components of the soil–plant–atmosphere continuum.

18
19
20 143 AquaCrop describes the soil as a reservoir split into several horizons (5 maximum). Each hori-
21
22 144 zon is characterized by texture or related hydrodynamic properties: soil moisture at field ca-
23
24 145 pacity (HFC), soil moisture at wilting point (HWP), soil moisture at saturation (HSAT), satu-
25
26 146 rated hydraulic conductivity (KSAT) and drainage coefficient (τ).

27
28
29
30
31 147 The model calculates soil evaporation (E_s) and crop transpiration (T_r) separately, which per-
32
33 148 mits the quantification of the amount of water unused by vegetation (Steduto et al., 2009).

34
35 149 Another feature of the model is the description of canopy growth by using canopy cover (CC)
36
37 150 instead of leaf area index (LAI). The model calculates T_r as a function of CC, and biomass is
38
39 151 determined as a function of both T_r and normalized water productivity (WP^*). The yield is
40
41 152 finally calculated by multiplying biomass by harvest index (HI). Water productivity (WP^*)
42
43 153 accounts for atmospheric concentration [CO_2] and therefore permit to apply AquaCrop in pro-
44
45 154 spective climate contexts related to precipitation, air temperature, evaporative demand and
46
47
48
49 155 [CO_2].

50
51
52
53 156 The soil water content at each time step results from the balance of drainage, infiltration from
54
55 157 rainfall/irrigation, soil evaporation and crop transpiration. AquaCrop accounts for four types
56
57
58 158 of stress that affect crop growth: water stress, heat stress, fertilization stress and salinity stress.

159 Depending on the type of stress, the target parameters of the model change. For example, water
160 stress affects leaf and CC expansion, root zone expansion, transpiration and the harvest index.
161 The main variables simulated by the model relate to crop productivity (canopy cover, dry
162 aboveground biomass and yield) and water balance (soil water content, runoff, infiltration,
163 drainage, capillary rise, soil evaporation and vegetation transpiration). The model parameters
164 are related to the crop (conservative parameters, fixed for a given species and nonconservative
165 parameters, varying according to the varieties), the soil (horizon number, texture or hydrody-
166 namic parameters), and the groundwater table (depth). The forcing variables of the model are
167 the climatic variables: reference evapotranspiration (ET_0), air temperature, rainfall and mean
168 annual $[CO_2]$. Agricultural practices include sowing date, fertilization and irrigation. Finally,
169 the initial conditions include the initial soil water and salinity content.

170 **3. Materials and methods**

171 **3.1. Study site**

172 The study was conducted within the Kamech catchment, which is the southern site of the Med-
173 iterranean Observatory of Rural Environment and Water (French acronym OMERE, Molénat
174 et al., 2018) that has collected multiple observations over the last 30 years. Kamech is a small
175 hilly catchment area (2.6 km² size) located within the Cap-Bon Peninsula, northeastern Tunisia
176 (10°52'-10°53'E and 36°52'-36°53' N, 108 m above sea level - asl.). It is representative of the
177 climatic and cropping conditions of the region. The climate is Mediterranean subhumid/semi-
178 arid. The rainy season spans from October to March (Mekki, 2003) with a cumulative rainfall
179 of 635 mm (annual average over the [1994-2020] period) and an annual reference evapotran-
180 spiration of 1366 mm (Molénat et al., 2018). The area is 70% agricultural, combining crops
181 and livestock, with significant spatiotemporal variability in land cover and spatial heterogene-
182 ity in soil types (Mekki, 2003; Mekki et al., 2006).

183 The Kamech catchment is typified by a diversified land cover that encompasses rainfed and
184 fodder crops (Mekki, 2003; Zitouna-Chebby et al., 2018). The dominant crops are winter cereals
185 (durum wheat, barley, oats and triticale) and legumes (chickpeas, faba bean and peas). Altitudes
186 range from 80 m to 200 m, and terrain slopes vary between 0 and 30%. The geological substratum
187 is from the Miocene epoch, and it is mainly made of marl and clay (Mekki, 2003; Molénat
188 et al., 2018). The four dominant soils are Cambisols, Luvisols, Vertisols and Regosols. They
189 cover 46%, 26%, 10% and 18% of the catchment area, respectively (Mekki et al., 2018b). The
190 soil depth varies from a few millimetres to 2 m.

191 Kamech is also typified by a large occurrence of swelling clay soils with shrinkage cracks that
192 occur from March to December (Mekki, 2003; Inoubli, 2016). The closing of cracks heavily
193 depends on rainfall at the beginning of the wet season and completely ends after cumulative
194 rainfalls of approximately 200 mm \pm 50 mm (Mekki, 2003). At their maximum opening, they
195 have a water storage capacity of approximately 70 mm. Runoff occurs from December to
196 March, when cracks are closed (Mekki, 2003; Inoubli, 2016).

197 **3.2. Datasets**

198 The current study benefits from a large database collected over the last three decades in the
199 framework of the OMERE Observatory. This database includes meteorological, pedological,
200 hydrological and agronomic observations (Mekki et al., 2006, 2018; Zitouna-Chebby et al.,
201 2018; Inoubli et al., 2017). This permitted to perform a thorough, multicriteria evaluation of
202 the AquaCrop model.

203 We chose wheat/barley, oats and faba bean as representative species of grain cereals, fodder
204 cereals and legumes, respectively. For each of these crops, some datasets were available be-
205 tween 2001 and 2013. Each of these datasets included a range of observations collected
206 throughout a crop cycle on a given plot from September to August that also corresponded to a

1
2
3
4
5
6
7
8
9
10
11
12
13
14
15
16
17
18
19
20
21
22
23
24
25
26
27
28
29
30
31
32
33
34
35
36
37
38
39
40
41
42
43
44
45
46
47
48
49
50
51
52
53
54
55
56
57
58
59
60
61
62
63
64
65

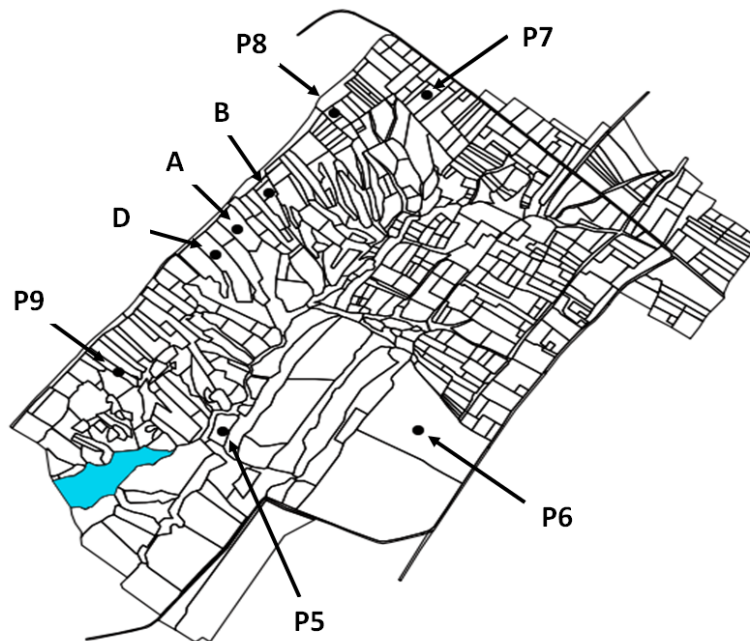
207 hydrological year. We selected the nine most complete datasets for conducting the AquaCrop
208 multicriteria evaluation. This resulted in the combination of five years and eight plots. Table 1
209 shows the available datasets, including the panel of data available in each of the nine datasets
210 for the AquaCrop multicriteria evaluation. Fig. 1 shows the location of the plots within the
211 Kamech catchment. In the panel of plots presented in Fig. 1, plot A differs from the others.
212 Indeed, this plot has been dedicated for two decades to regular monitoring as part of the
213 OMERE Observatory. This monitoring included meteorological forcing, surface and subsur-
214 face hydrological monitoring, vegetation monitoring and soil characterization.

215 In the remainder of this section, we present the climatic, pedological, agronomic and hydrolog-
216 ical data, by distinguishing between (1) the data used as inputs to the AquaCrop model and
217 (2) the data used for the multicriteria evaluation of the model simulations.

218

219 **Table 1.** The nine available datasets for the multicriteria evaluation of AquaCrop. *LAI_plan*,
 220 *CC_visu*, *ET_a*, *R* and *SWC* stand for *LAI* from planimetric measurements, canopy cover from
 221 visual quantification, actual evapotranspiration, runoff and soil water content, respectively.
 222 The value *Y* of the label Year is related to harvesting year, and thus corresponds the crop cy-
 223 cle that spreads from September of year *Y-1* to August of year *Y*.

Crop	Dataset		Available data					
	Year	Plot	LAI_plan	CC_visu	ET _a	R	SWC	AGB
Wheat	2001	P7	x			x	x	x
	2002	P9	x			x	x	x
	2013	A	x		x	x	x	x
Barley	2006	D	x				x	
Oats	2002	P6	x			x	x	x
	2005	B	x		x		x	x
Faba	2001	P5		x		x	x	x
	2001	P8		x		x	x	x
	2002	P7		x		x	x	x



224
 225 **Fig. 1.** Map of the Kamech catchment with the location of the plots A, B, D, P5, P6, P7, P8
 226 and P9. The meteorological station is located near the outlet of the catchment area, down-
 227 stream limit of the hilly lake.

228 3.2.1. AquaCrop input data

229 3.2.1.1. Climatic data

1
2
3 230 The climatic data were collected by the meteorological station located near the outlet of the
4
5 231 catchment area (see Fig. 1). First, ET_0 was calculated at the half-hourly time step by using the
6
7
8 232 FAO-56 method along with measurements of solar radiation, air temperature, air humidity and
9
10 233 wind speed. Next, estimates calculated at the half-hourly time step were integrated at the daily
11
12 234 timescale.

13
14
15 235 All rainfall data were collected at a daily time step. The rain gauge for each of the plots P5, P6,
16
17
18 236 P7, P8 and P9 was located downstream of the plot. For plots A, B and D, we used the data
19
20 237 collected by the rain gauge located downstream of plot A, thanks to their spatial proximity. In
21
22
23 238 the case of missing data, we used average values across all rain gauges within the catchment
24
25 239 area.

240 3.2.1.2. Soil hydrodynamic parameters

241 AquaCrop inputs include soil depth and soil moisture at wilting point (HWP) and at field ca-
242 capacity (HFC). We consider three soil classes: Vertisols for plots A, B, D and P5, Cambisols for
243 plots P6, P7, and P8 and Luvisols for plot P9. Soil depth and hydrodynamic parameters for
244 each plot are shown in Table 2.

245 We summarize in this section the estimation of HWP and HFC; a detailed description is pro-
246 vided in Section 1 of the supplementary materials. We used the laboratory measurements (Cas-
247 sel and Nielsen, 1986) conducted within the framework of the OMERE Observatory, and the
248 agroclimatic method (Sreelash et al., 2017) with discrete soil moisture measurements con-
249 ducted at specific dates. The comparison of the estimates resulting from these two approaches
250 showed relative differences of approximately 15% on average (Table SP1 in supplementary
251 materials), which corresponds to the precision and spatial representativeness of local field
252 measurements, approximately 15% (Susha Lekshmi et al., 2014; Walker et al., 2004; Robinson

253 et al., 2008). Next, we verified the consistency of the HWP and HFC estimates with the time
 1
 2 254 series of SWC (SWC data are presented in Section 3.3.6). This led to the use of the estimates
 3
 4
 5 255 from the laboratory measurements for plot A, and to the estimates from the agroclimatic
 6
 7 256 method for the other plots.

10 257 **Table 2.** *Soil characteristics of the plots. Soil classes are taken from Mekki et al. (2006). We*
 11
 12
 13 258 *used the same values of soil depth for plots A, B and D thanks to their spatial proximity.*

Plot	Class	Soil depth	Soil hydrodynamic parameters (m ³ /m ³)	
			HWP	HFC
P5	Vertisol	1.60	0.23	0.45
P6	Cambisol	1.50	0.21	0.35
P7	Cambisol	1.60	0.23	0.44
P8	Cambisol	1.20	0.19	0.46
P9	Luvisol	1.60	0.25	0.47
A	Vertisol	1.15	0.34	0.43
B	Vertisol	1.15	0.26	0.44
D	Vertisol	1.15	0.23	0.44

30 260 3.2.1.3. Crop parameters

31
 32
 33 261 We chose wheat/barley, oats and faba bean as representative species of grain cereals, fodder
 34
 35 262 cereals and legumes, respectively. In the literature, there are some annual crops for which Aq-
 36
 37
 38 263 uaCrop parameterizations are not representative of various agro-environmental conditions. In-
 39
 40 264 deed, some parameterizations are proposed in the literature for chickpeas (Mubvuma et al.,
 41
 42
 43 265 2021), leafy vegetables (Nyathi et al., 2018), table grape (Er-Raki et al., 2021), oats and faba
 44
 45 266 bean (Yuan et al., 2013; Zeleke, 2019), but they need to be tested and confirmed in other geo-
 46
 47
 48 267 climatic contexts and for other crop varieties to ensure that they are reliable, as is the case for
 49
 50 268 those related to wheat or corn crops.

51
 52
 53 269 For wheat, barley and faba bean, we used parameters proposed in the literature that were rather
 54
 55 270 suitable for the local varieties of our study site, as indicated in Table 2 of Alaya et al. (2019).
 56
 57
 58 271 For oats, we used the values proposed by Yuan et al. (2013) for the conservative parameters
 59
 60
 61
 62
 63
 64
 65

272 (invariant from one variety to another), and we used values related to wheat for the noncon-
273 servative parameters that describe the phenological stages throughout the crop cycle, due to the
274 lack of data.

275 **3.2.2. AquaCrop multicriteria assessment**

276 **3.2.2.1. Actual evapotranspiration (ET_a)**

277 For actual evapotranspiration, two datasets were available (Table 1): the first dataset was col-
278 lected in plot A in 2013 for wheat, and the second dataset was collected in plot B in 2005 for
279 oats. The time series were collected at the plot scale, with a 30 min timescale throughout the
280 crop cycle. The daily ET_a measurements were derived from the energy balance closure method
281 in 2005 (Zitouna-Chebbi et al., 2015) and from the eddy covariance method in 2013 (Boudhina
282 et al., 2017a). For 2013, the missing latent heat flux data were reconstructed using the REddy-
283 Proc gap-filling method (Reichstein et al., 2005). The experimentation, calibration, data pro-
284 cessing and gap-filling are discussed in detail by Zitouna-Chebbi (2009); Zitouna-Chebbi et
285 al., (2012; 2015; 2018), and Boudhina et al., (2017a, 2017b, 2018). ET_a data were finally ag-
286 gregated at the daily timescale.

287 **3.2.2.2. Crop variables (CC, AGB)**

288 When dealing with vegetation growth throughout the crop cycle, we used planimetric meas-
289 urements of the leaf area index (LAI) for cereals (wheat, barley, oats) and visual estimates of
290 canopy cover (CC) for faba bean (Table 1). Nevertheless, AquaCrop simulates CC to describe
291 crop growth. For cereals, we therefore converted LAI measurements into CC estimates by using
292 Equation 1, as done in numerous studies (Katerji et al., 2013; Yuan et al., 2013; Pereira et al.,
293 2015):

$$294 \quad CC = 1 - e^{-k \times LAI} \quad (\text{Equation 1})$$

1
2
3
4
5
6
7
8
9
10
11
12
13
14
15
16
17
18
19
20
21
22
23
24
25
26
27
28
29
30
31
32
33
34
35
36
37
38
39
40
41
42
43
44
45
46
47
48
49
50
51
52
53
54
55
56
57
58
59
60
61
62
63
64
65

295 Coefficient k is an extinction coefficient that quantifies the light interception by canopy cover
296 (Pereira et al., 2015). We used a k value equal to 0.57 for all cereals. The determination of this
297 k value is discussed in Section 2 of the supplementary materials.

298 We also used measurements of dry aboveground biomass (AGB), except for barley in plot D
299 in 2006. For each of the eight datasets, AGB was determined throughout the crop cycle using
300 a destructive method (i.e., field samples to be weighed before and after oven drying). Spatial
301 sampling varied across datasets, ranging from three to 10 replicates (Mekki, 2003; Boudhina
302 et al., 2019). For each crop, the number of observation dates also varied across datasets, be-
303 tween three and 11 dates at maximum.

304 **3.2.2.3. Soil water content (SWC)**

305 Time series of SWC measurements were available for all datasets (Table 1). For 2001, 2002
306 and 2013, measurements were made using a neutron probe with a weekly frequency. For 2005
307 and 2006, measurements were made by the gravimetric method, with a biweekly frequency
308 throughout the crop cycle and with a bimonthly frequency during summer with bare soil. All
309 measurements were carried out across 1 m depth profiles. To account for spatial variability in
310 SWC, the samples were collected at different landscape positions (distributed across the top,
311 middle and bottom of each plot), except for 2001 and 2002, with one measurement only per
312 plot. The moisture values were obtained by plot-scale averaging of measurements. Detailed
313 descriptions of the measurements are given in Mekki (2003); Zitouna-Chebbi (2009); Boudhina
314 et al. (2019).

315 **3.2.2.4. Runoff (R)**

316 Runoff measurements were included in each of the datasets listed in Table 1, apart from oats
317 in 2005 and barley in 2006. Runoff data were collected at the daily timescale.

- 318 • For 2001 (end of December) and 2002 (November), runoff was measured in each plot using
 319 a 2 m² size harvesting frame that was connected to a tank with a 20-litre capacity (Mekki
 320 et al., 2006).
- 321 • For 2013, runoff was measured by the hydrological station located at the outlet of plot A.
 322 The experimental protocol is detailed in Inoubli et al. (2017).

323 3.3. Determination of initial soil moisture and fertilization degree

324 To obtain reliable AquaCrop simulations throughout the crop cycle for each of the nine datasets
 325 (Table 1), it was necessary to set the initial soil water content (SWC_i). It was also necessary to
 326 set the fertilization rate (FR) for cereal crops, while no fertilization rate was required for faba
 327 bean that is a nitrogen-fixing legume crop (FR represents the effect of the soil nutrient level on
 328 canopy development and biomass production, and AquaCrop expresses the lack of soil nutrient
 329 from soil fertility stress, by means of stress coefficients). Given that no information was avail-
 330 able for either SWC_i or FR, we determined them by minimizing the differences between ob-
 331 servations and simulations of CC, AGB and SWC (time series of ET_a were available for only
 332 two datasets).

333 For each of the nine datasets, we choose 15 SWC_i values between HWP and HFC and 30 FR
 334 values ranging from 70 to 100% according to expert knowledge. We then created pairs (SWC_i,
 335 FR) and generated the corresponding AquaCrop simulations. The optimal (SWC_i, FR) pair was
 336 selected using two criteria. First, the NRMSE (normalized root mean square error) had to be
 337 lower than 15% for SWC, which corresponds to measurement error on soil moisture (Susha
 338 Lekshmi et al., 2014). Second, we minimized the quadratic error between the observations and
 339 simulations of CC and AGB simultaneously using the objective function F defined by Equation
 340 2 (Montes et al., 2014):

$$341 \quad F = \text{NRMSE}_{\text{CC}}^{1/2} + \text{NRMSE}_{\text{AGB}}^{1/2} \quad (\text{Equation 2})$$

1
2
3
4
5
6
7
8
9
10
11
12
13
14
15
16
17
18
19
20
21
22
23
24
25
26
27
28
29
30
31
32
33
34
35
36
37
38
39
40
41
42
43
44
45
46
47
48
49
50
51
52
53
54
55
56
57
58
59
60
61
62
63
64
65

342 AquaCrop tends to overestimate CC observations during the senescence phase in the case of
343 heat waves (Andarzian et al., 2011), while early senescence is recurrent in Kamech. To avoid
344 the influence of any overestimation when minimizing the quadratic error, we calculated F over
345 a simulation period that spread from the beginning of the crop growth to the maximum plant
346 cover ($CC = CC_{max}$). Across the selected AquaCrop simulations, the obtained SWC_i values
347 were larger than $0.75 \times HFC$, and those retained for FR were approximately 85%. According
348 to expert opinions, the FR values are representative of actual field conditions in the Kamech
349 watershed.

350 3.4. Model evaluation

351 AquaCrop was evaluated by comparing simulations against observations throughout the crop
352 cycle related to each of the nine datasets by considering the variables listed in Table 1 and
353 related to vegetation (AGB, CC), water fluxes (ET_a , runoff as infiltration excess), and water
354 storage (SWC). Table 1 details the available data used for each crop, year and plot.

355 For the statistical evaluation of the simulations against observations, we selected the following
356 indicators: coefficient of determination (R^2), root mean square error (RMSE), normalized root
357 mean square error (NRMSE) and mean bias error (MBE). These are commonly used in the
358 literature for evaluating numerical models (Kustas et al., 1996; Jacob et al., 2002), including
359 hydrological (Moriassi et al., 2015) or crop (Yang et al., 2014) models. We also used the Stu-
360 dent's t test for linear regressions on model validation, to test the null hypothesis (slope and
361 offset can be equal to 1 and 0, respectively). If the critical values (p value) were larger than
362 5%, then the null hypothesis could not be rejected with 95% confidence, and model perfor-
363 mances could be considered satisfactory.

$$R^2 = \frac{\sum_{i=1}^n (P_i - \bar{O})^2}{\sum_{i=1}^n (O_i - \bar{O})^2} \quad (\text{Equation 3})$$

$$RMSE = \sqrt{\frac{\sum_{i=1}^n (P_i - O_i)^2}{n}} \quad (\text{Equation 4})$$

$$NRMSE = \frac{RMSE}{\bar{O}} \times 100 \quad (\text{Equation 5})$$

$$MBE = \frac{\sum_{i=1}^n (P_i - O_i)}{n} \quad (\text{Equation 6})$$

where P_i and O_i , are the simulated and observed variables at time step i , respectively. \bar{O} is the averaged value of the observations, and n is the observation number.

MBE indicates whether the model simulations underestimate or overestimate the observations.

NRMSE gives an indication of the relative difference between simulations and observations.

According to Jamieson et al. (1991), a crop model is classified as excellent if $NRMSE < 10\%$,

good if $NRMSE \in [10\% - 20\%[$, acceptable if $NRMSE \in [20\% - 30\%[$ and poor if $NRMSE >$

30% . Likewise, simulations are considered acceptable if the coefficient of determination R^2 is

greater than 0.5. For runoff, we did not consider the NRMSE in the evaluation of the AquaCrop

simulations because of the low values of this variable, which give very high NRMSE values ($>$

100%) that are difficult to interpret.

4. Results

4.1. Canopy cover (CC)

According to the comparison between AquaCrop simulations and in situ measurements of CC

(Fig. 2 and Table 3), for each crop type, AquaCrop simulations overestimated observations for

cereals and underestimated them for faba bean, with a positive MBE ranging between 0.03 and

0.23 for cereals and a negative MBE (-0.02) for faba bean. The R^2 values did not exceed 0.4,

apart from faba bean (0.9). The RMSE values varied between 0.11 (29% relative) and 0.37

(75% relative), with the lowest values being observed for faba bean. For wheat and faba bean,

the t test provided p values larger than 5% on slope and offset. For barley, the t test provided p

1 383 value lower than 5% on slope and offset. For oats, the t test provided a p value lower than 5%
2 384 on offset only.

3
4
5 385 To study these results in detail, we analysed the temporal evolution of CC for each simulation
6
7 386 throughout the corresponding crop cycle (Fig. SP2 in Section 3 of the supplementary materi-
8
9 387 als). For wheat in 2002, oats in 2005, and barley in 2006, the temporal evolution of the canopy
10
11 388 cover simulated by the model showed acceptable estimates during the crop growth phase, de-
12
13 389 spite an overestimation of CC observations during the senescence phase. For wheat in 2013,
14
15 390 AquaCrop underestimated observations between DAS (day after sowing) 25 and DAS 120, and
16
17 391 it overestimated them at the end of the crop cycle. For oats in 2002, the model underestimated
18
19 392 observations throughout the crop cycle. Most time series suggested that AquaCrop simulated
20
21 393 senescence with delay compared to observations.
22
23
24
25
26
27

28 394
29
30
31
32
33
34
35
36
37
38
39
40
41
42
43
44
45
46
47
48
49
50
51
52
53
54
55
56
57
58
59
60
61
62
63
64
65

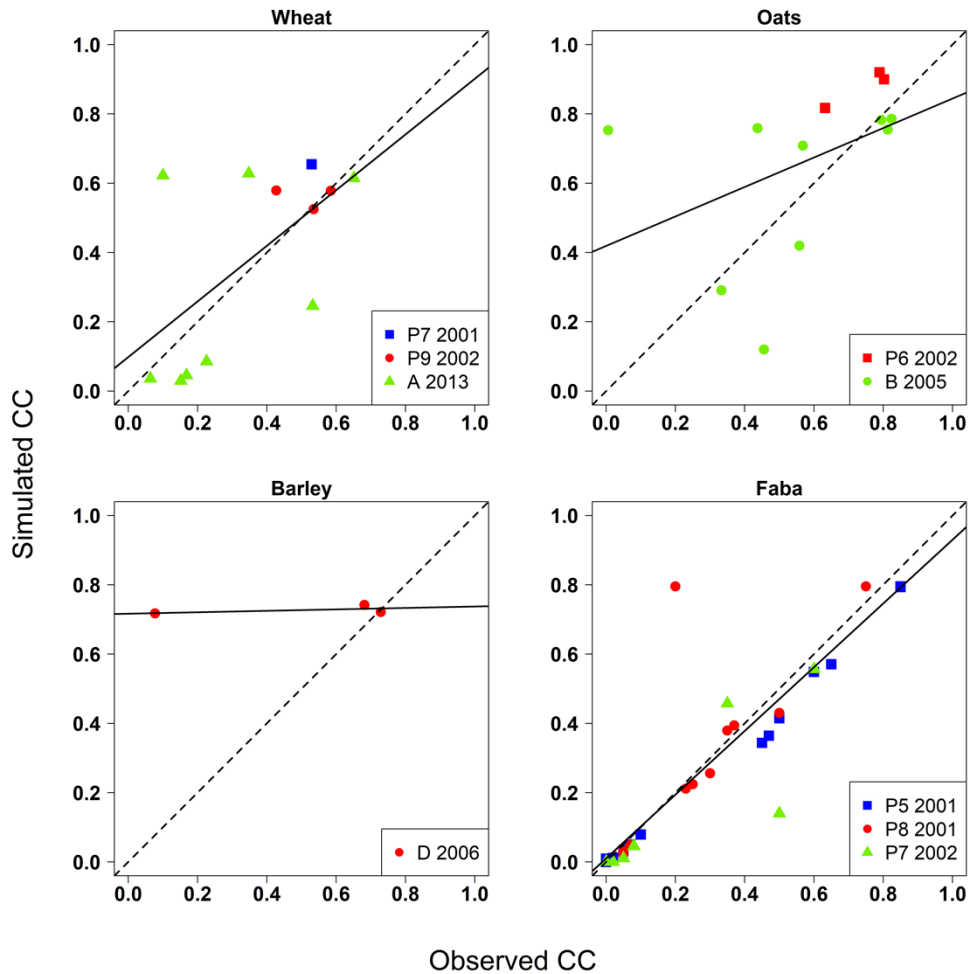


Fig. 2. Comparison between simulated and observed canopy cover (CC) on a crop type basis.

Each scatterplot corresponds to a crop type for several years and/or several plots. Each dataset is indicated by a different marker and a different colour. Px, A, B, D relates to plots and YYYY to years. The black line corresponds to the regression line, and the black dashed line corresponds to the 1:1 line.

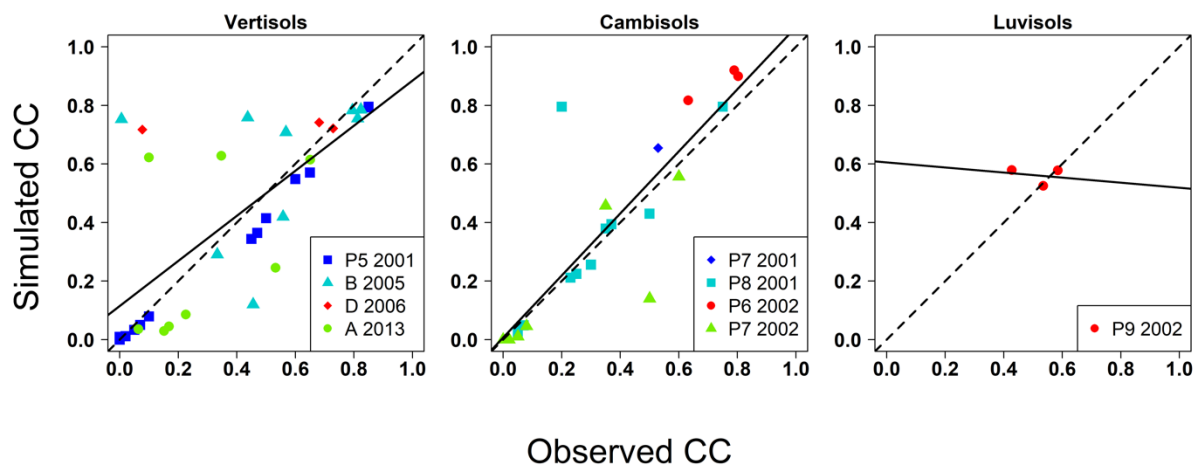
Table 3. Statistical indicators when comparing simulations against observations for canopy cover (CC) on a crop type basis. n is the observation number. R^2 is the correlation coefficient. The t test corresponds to the p value of the Student's t test. The statistical indicators RMSE, NRMSE and MBE are defined in Section 3.4.

Crop	Var	n	R^2 (-)	Offset	Slope	RMSE (-)	NRMSE (%)	MBE (-)
				(-)	(-)			
				Value	t test	Value	t test	

Wheat	CC	12	0.39	0.10	0.47	0.80	0.55	0.21	58	0.03
Oats		12	0.18	0.42	0.04	0.43	0.08	0.27	46	0.08
Barley		3	0.33	0.72	0.02	0.02	0.02	0.37	75	0.23
Faba		38	0.86	0.01	0.73	0.92	0.21	0.12	32	-0.02

For each soil class, the comparison between AquaCrop simulations and in situ measurements of CC (Fig. 3 and Table 4) showed that AquaCrop simulations overestimated observations for the three soil classes. Additionally, the agreement between the model simulations and in situ measurements was moderate, with either (1) large R^2 values (0.59 and 0.8) but large RMSE values (0.15 and 0.21, corresponding to 41% and 48% relative, respectively) or (2) a moderate RMSE value (0.09, 18% relative) but a low R^2 value (0.05). Nevertheless, it was difficult to conclude for Luvisols because of the dataset size, with only one plot and one year. Conversely, the results for both Vertisols and Cambisols were similar, with relative changes in statistical indicators of approximately 25%. Apart from t test on slope for Vertisols, all p values were larger than 5%.

Finally, we could not conclude on any possible trend to over- or under- estimation according to the magnitude of observations. Indeed, the regression slope could be larger or lower than one from one soil class to another, in contrast to results reported on a crop type basis for which the regression slope was systematically lower than one.



421 **Fig. 3** Comparison between simulated and observed canopy cover (CC) on a soil class basis.
 422 Each scatterplot corresponds to a soil class for several plots, years and crops. Each dataset
 423 is indicated by a different marker and a different colour. Px, A, B, D relates to plots and
 424 YYYY to years. The black line corresponds to the regression line, and the black dashed line
 425 corresponds to the 1:1 line.

426 **Table 4.** Statistical indicators when comparing simulations against observations for canopy
 427 cover (CC) on a soil class basis. n is the observation number. R^2 is the correlation coeffi-
 428 cient. The t test corresponds to the p value of the Student's t test. The statistical indicators
 429 RMSE, NRMSE and MBE are defined in Section 3.4.

Soil	Var	n	R^2 (-)	Offset		Slope		RMSE (-)	NRMSE (%)	MBE (-)
				Value	t test	Value	t test			
Vertisols	CC	39	0.59	0.12	0.05	0.77	0.03	0.21	47	0.01
Cambisols		23	0.76	0.01	0.90	1.06	0.64	0.16	45	0.03
Luvisols		3	0.05	0.61	0.20	-0.09	0.21	0.09	17	0.05

430 4.2. Aboveground biomass (AGB)

431 The comparison between simulated and observed AGB (Fig. 4 and Table 5), for each crop type,
 432 showed a good estimation of this variable by the model for cereals, with R^2 approximately 0.95
 433 and RMSE approximately 0.6 ton ha⁻¹ (16% relative). For faba bean, the simulations were less
 434 good, with $R^2 = 0.52$ and RMSE = 1.4 ton ha⁻¹ (46% relative). The bias values indicated that
 435 AquaCrop tended to overestimate AGB observations for cereals (MBE > 0) and to underesti-
 436 mate them for faba bean (MBE < 0). For all crop types, the t test provided p values larger than
 437 5%.

438

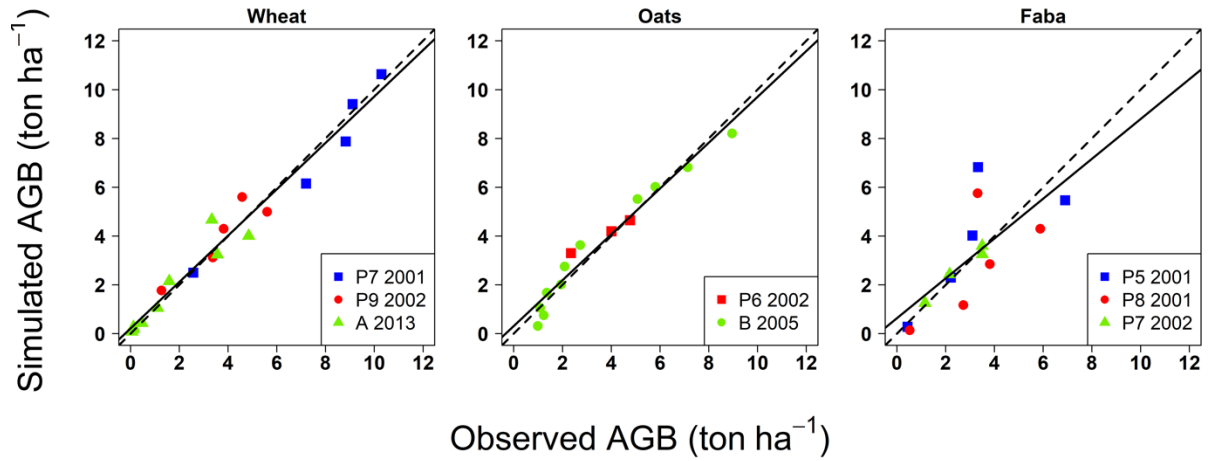


Fig. 4. Comparison between simulated and observed aboveground biomass (AGB) on a crop type basis. Each scatterplot corresponds to a crop type for several years and/or several plots. Each dataset is indicated by a different marker and a different colour. Px, A, B, D relates to plots and YYYY to years. The black line corresponds to the regression line, and the black dashed line corresponds to the 1:1 line.

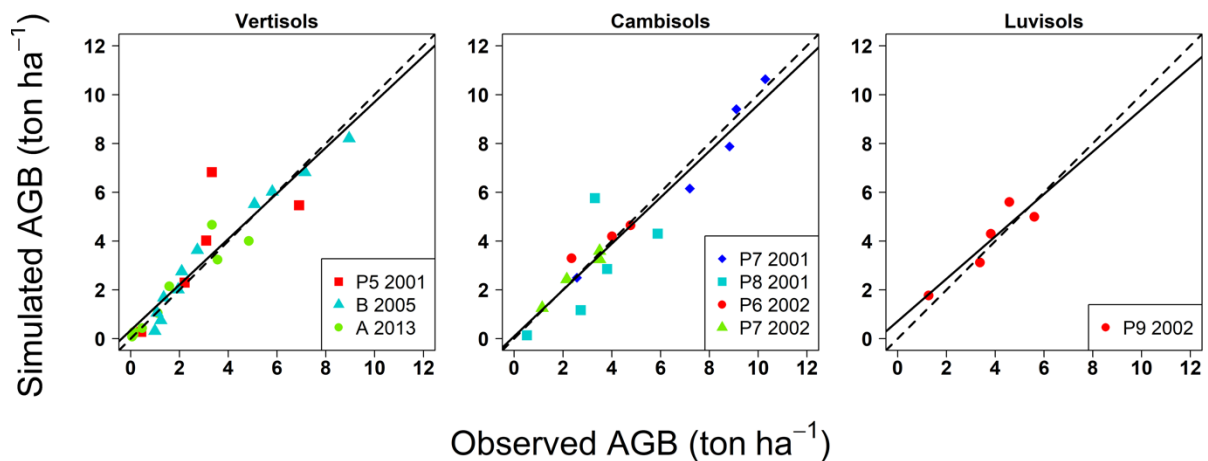
Table 5. Statistical indicators when comparing simulations against observations for aboveground biomass (AGB) on a crop type basis. *n* is the observation number. R^2 is the correlation coefficient. The *t* test corresponds to the *p* value of the Student's *t* test. The statistical indicators RMSE, NRMSE and MBE are defined in Section 3.4.

Crop	Var	n	R^2 (-)	Offset (ton ha ⁻¹)		Slope (-)		RMSE (ton ha ⁻¹)	NRMSE (%)	MBE (ton ha ⁻¹)
				Value	t test	Value	t test			
				Wheat	AGB	19	0.96			
Oats		14	0.95	0.31	0.25	0.94	0.33	0.53	15	0.10
Faba		14	0.52	0.64	0.44	0.82	0.43	1.40	46	0.08

To better understand the poor results for faba bean, Fig. SP3 displays the temporal evolution of AGB for both cereal crops and faba bean during the crop cycle. We noted that AquaCrop appropriately simulated AGB for 2002 in plot P7. For the year 2001 in plots P5 and P8, the model acceptably simulated AGB at the beginning of the crop cycle until Day 125 after sowing,

453 but it overestimated observations at the end of the crop cycle. This could explain the low R^2
 454 value given in Table 5.

455 The comparison between AquaCrop simulations and in situ measurements of AGB (Fig. 5 and
 456 Table 6) for each soil class, showed that AquaCrop simulated AGB well for the 3 soil classes.
 457 Bias values indicated that the model tended to overestimate observations for Vertisols and Lu-
 458 visols ($MBE > 0$) and to underestimate them for Cambisols ($MBE < 0$). The R^2 values were
 459 above 0.84, with a small relative variation of 6% across the 3 soil classes. The RMSE values
 460 were between 0.62 ton ha^{-1} (17% relative) and 0.95 ton ha^{-1} (21% relative). Additionally, all
 461 regression slopes were close to one, as was the case when analysing results on a crop type basis.
 462 This outcome agreed with the results of the t test that provided p values larger than 5% for all
 463 soil classes.



465

466 **Fig. 5.** Comparison between simulated and observed aboveground biomass (AGB) on a soil
 467 class basis. Each scatterplot corresponds to a soil class for several plots, years and crops.
 468 Each dataset is indicated by a different marker and a different colour. Px, A, B, D relates to
 469 plots and YYYY to years. The black line corresponds to the regression line, and the black
 470 dashed line corresponds to the 1:1 line.

471 **Table 6.** Statistical indicators when comparing simulations against observations for above-
 472 ground biomass (AGB) on a soil class basis. n is the observation number. R^2 is the correla-
 473 tion coefficient. The t test corresponds to the p value of the Student's t test. The statistical in-
 474 dicators RMSE, NRMSE and MBE are defined in Section 3.4.

Soil	Var	n	R^2 (-)	Offset (ton ha ⁻¹)		Slope (-)		RMSE (ton ha ⁻¹)	NRMSE (%)	MBE (ton ha ⁻¹)
				Value	t test	Value	t test			
				Vertisols	AGB	25	0.86			
Cambisols		17	0.89	0.10	0.83	0.95	0.56	0.95	21	-0.13
Luvisols		5	0.84	0.72	0.47	0.87	0.59	0.62	17	0.23

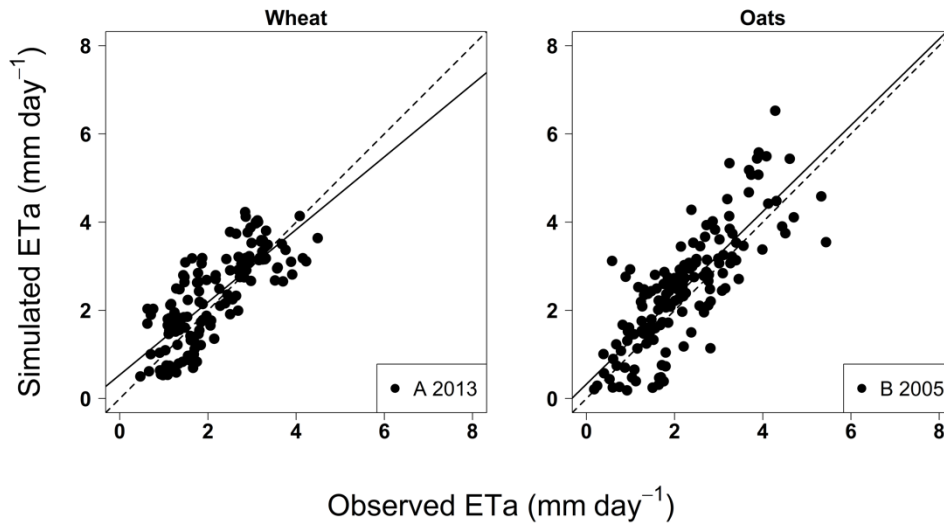
475 4.3. Actual evapotranspiration (ET_a)

476 As shown in Table 1, ET_a measurements were only available for oats in 2005 (plot B) and for
 477 wheat in 2013 (plot A). The comparison between AquaCrop simulations and in situ measure-
 478 ments of ET_a (Fig. 6 and Table 7) showed a slight overestimation of the observations. The
 479 overestimation was more important for oats (MBE = 0.28 mm day⁻¹) than for wheat
 480 (MBE = 0.17 mm day⁻¹). The other indicators showed that the model performance was accepta-
 481 ble for both crops, with $R^2 \geq 0.6$ and $RMSE \leq 0.84$ mm day⁻¹ (35% relative on average). Addi-
 482 tionally, we noted scatterings around the regression lines that were close to the 1:1 line. Apart
 483 from slope for wheat, the t test provided p values lower than 5%.

484 **Table 7.** Statistical indicators when comparing simulations against observations for actual
 485 evapotranspiration (ET_a) on a crop type basis. n is the observation number. R^2 is the correla-
 486 tion coefficient. The t test corresponds to the p value of the Student's t test. The statistical in-
 487 dicators RMSE, NRMSE and MBE are defined in Section 3.4.

Crop	Var	n	R^2 (-)	Offset (mm day ⁻¹)		Slope (-)		RMSE (mm day ⁻¹)	NRMSE (%)	MBE (mm day ⁻¹)
				Value	t test	Value	t test			
				Wheat	ET _a	134	0.59			
Oats		150	0.64	0.33	0.03	0.98	0.72	0.84	38	0.28

488



489

490 **Fig. 6.** Comparison between simulated and observed actual evapotranspiration (ET_a) on a
491 crop type basis. Each scatterplot corresponds to a crop type. A, B relates to plots and YYYY
492 to years. The black line corresponds to the regression line, and the black dashed line corre-
493 sponds to the 1:1 line.

494 For a better understanding of the scattering around the regression line, we investigated the
495 temporal dynamics of ET_a simulations by AquaCrop throughout the crop cycle for wheat and
496 oats (Fig. SP4). We observed a significant similarity between the simulated and observed tem-
497 poral evolutions of ET_a for both crops. For wheat, the overestimation of ET_a observations by
498 model simulations was more important from DAS 130 (9 Mar 2013). For oats, we observed an
499 overestimation of ET_a observations by the model between DAS 140 – (3 May 2005) and DAS
500 160 - (23 May 2005) – as well as an underestimation of the observations from DAS 160 until
501 the end of the crop cycle. Overall, we did not observe any trend to under- or overestimation
502 according to crop phenological stages.

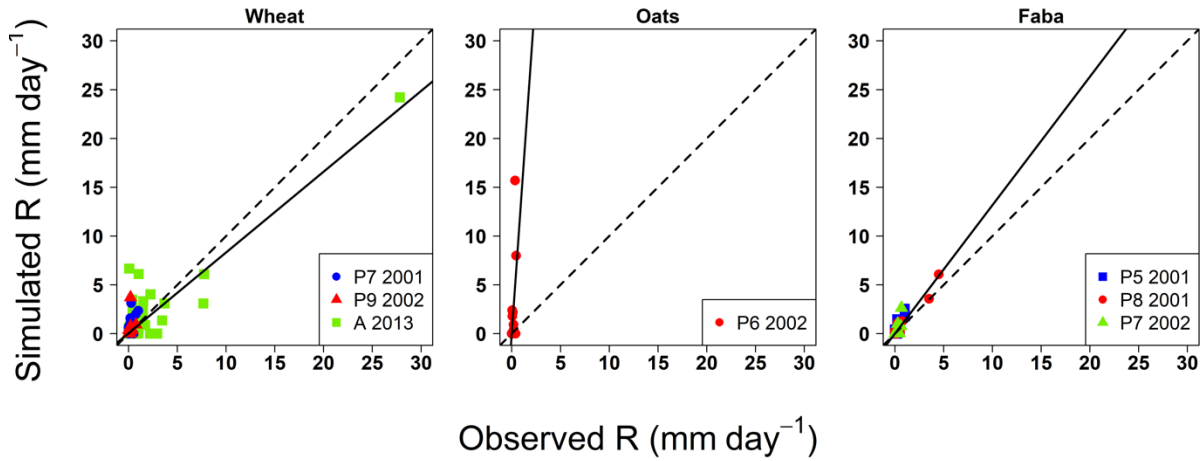
503 The two datasets of ET_a belonged to the Vertisols class. The statistical indicators we obtained
504 when merging the scatterplots in Fig. 6 suggested good model performance in simulating ET_a ,

1
2
3
4
505 with acceptable values for the correlation coefficient (0.62) and RMSE (0.77 mm day⁻¹) and a
506 slight overestimation of ET_a observations by model simulations (MBE = 0.23 mm day⁻¹).

507 4.4. Runoff (R)

508 For runoff (infiltration excess), in situ measurements were available for all datasets, except for
509 barley in plot D in 2006 and oats in plot B in 2005 (Table 1). The comparison between Aqua-
510 Crop simulations and in situ measurements (Fig. 7 and Table 8) for each crop type showed that
511 the model overestimated observations. The magnitude of the overestimation varied from one
512 crop to another, and it was larger for oats (MBE = 0.2 mm day⁻¹). AquaCrop acceptably simu-
513 lated runoff for wheat and faba bean, with R² values larger than 0.8 and RMSE values lower
514 than 0.63 mm day⁻¹. The simulations were less effective for oats (R² = 0.41; RMSE =
515 1.44 mm day⁻¹). According to Fig. 7, the overestimation of runoff observations by AquaCrop
516 simulations mainly occurred for low runoff values. For wheat in 2013 in plot A, the model
517 acceptably simulated a significant runoff event (27 mm day⁻¹) with a slight underestimation.
518 For all crops, the t test on slope provided p values equal to 0. Apart from wheat, the t test on
519 offset provided p values larger than 5%.

520



521

522

Fig. 7. Comparison between simulated and observed runoff (R) on a crop type basis. Each scatterplot corresponds to a crop type for several years and/or several plots. Each dataset is indicated by a different marker and a different colour. Px, A, B, D relates to plots and YYYY to years. The black line corresponds to the regression line, and the black dashed line corresponds to the 1:1 line.

527

Table 8. Statistical indicators when comparing simulations against observations for runoff (R) on a crop type basis. n is the observation number. R² is the correlation coefficient. The t test corresponds to the p value of the Student's t test. The statistical indicators RMSE, NRMSE and MBE are defined in Section 3.4.

530

Crop	Var	n	R ² (-)	Offset (mm day ⁻¹)		Slope (-)		RMSE (mm day ⁻¹)	MBE (mm day ⁻¹)
				Value	t test	Value	t test		
Wheat	R	478	0.80	0.06	0.03	0.83	0	0.63	0.02
Oats		147	0.41	-0.03	0.76	14.26	0	1.44	0.20
Faba		453	0.84	0.01	0.25	1.32	0	0.19	0.02

531

For a better understanding of these scatterplots, Fig. SP5 displays the temporal evolution of observed and simulated runoff for each dataset. Apart from wheat in plot A in 2013, the observed runoff was usually low, with values below 15 mm day⁻¹. The most important differences between observed and simulated accumulations were noted for wheat in plot P7 in 2001 (12

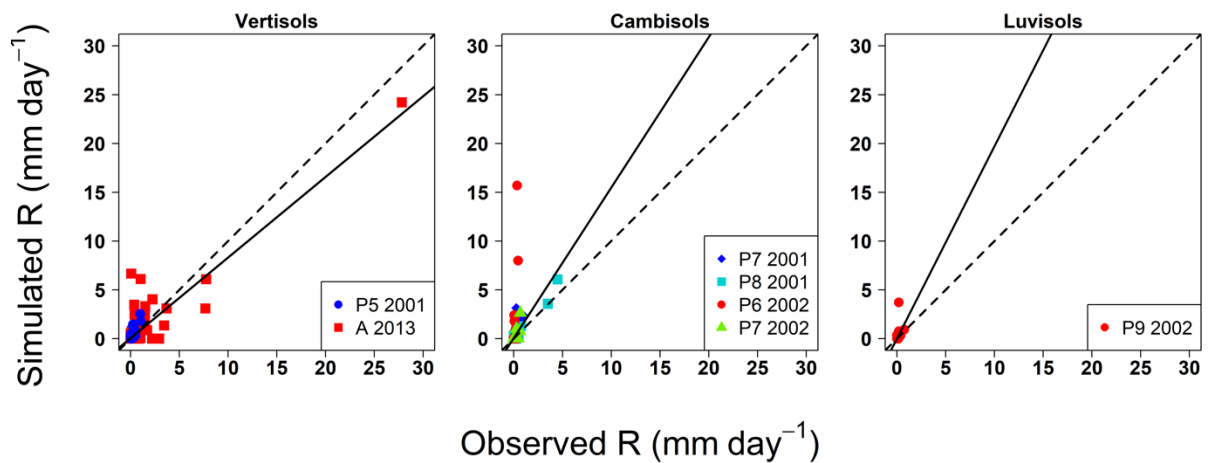
532

533

534

535 mm day⁻¹) and for oats in plot P6 in 2002 (29 mm day⁻¹). We also noted that the model simu-
 536 lated large runoff values at the beginning of the crop cycle compared to in situ measurements.
 537 This was true for wheat in plot P9 in 2002 and in plot A in 2013, as well as for oats in plot P6
 538 and faba bean in plot P7 in 2002. The same trend was also observed at the end of the crop cycle
 539 (the last 40 days) for oats in plot P6 in 2002 and wheat in plot A in 2013.

540 From the comparison between AquaCrop simulations and in situ measurements of runoff, for
 541 each soil class (Fig. 8 and Table 9) we noted a better performance of the model for Vertisols
 542 ($R^2 = 0.82$, RMSE = 0.71 mm day⁻¹), where the large R^2 value for Vertisols likely results from
 543 a single large runoff event. The model performed worse for Cambisols ($R^2 = 0.22$ and
 544 RMSE = 0.76 mm day⁻¹) and Luvisols ($R^2 = 0.21$ and RMSE = 0.28 mm day⁻¹). The t test pro-
 545 vided p values larger than 5% and lower than 5% for offset and slope, respectively.



547
 548 **Fig. 8.** Comparison between simulated and observed runoff (R) on a soil class basis. Each
 549 scatterplot corresponds to a soil class for several plots, years and crops. Each dataset is indi-
 550 cated by a different marker and a different colour. Px, A, B, D relates to plots and YYYY to
 551 years. The black line corresponds to the regression line and the black dashed line corre-
 552 sponds to the 1:1 line.

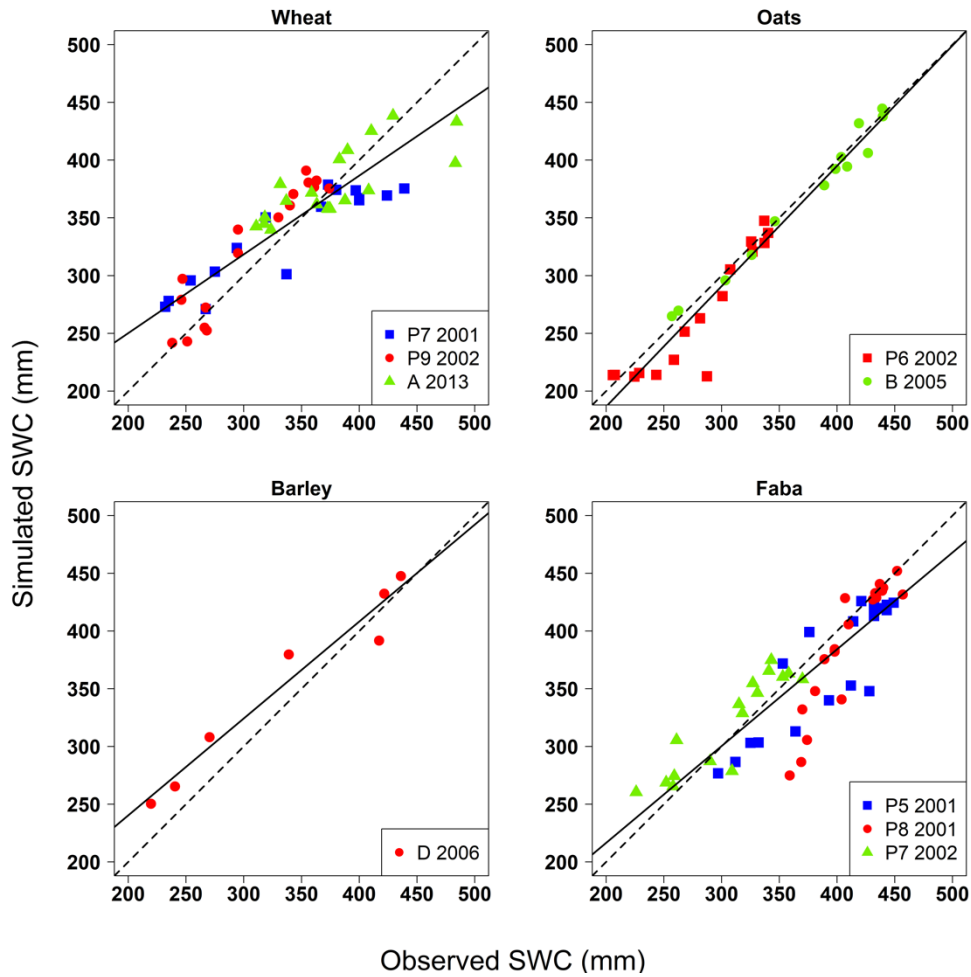
553 **Table 9.** Statistical indicators when comparing simulations against observations for runoff
 554 (*R*) on a soil class basis. *n* is the observation number. R^2 is the correlation coefficient. The *t*
 555 test corresponds to the *p* values of the Student's *t* test. The statistical indicators RMSE,
 556 NRMSE and MBE are defined in Section 3.4.

Soil	Var	n	R^2 (-)	Offset (mm day ⁻¹)		Slope (-)		RMSE (mm day ⁻¹)	MBE (mm day ⁻¹)
				Value	t test	Value	t test		
Vertisols	R	331	0.82	0.05	0.15	0.83	0	0.71	0.01
Cambisols		587	0.22	0.06	0.07	1.54	0	0.76	0.08
Luvisols		160	0.21	0.01	0.61	1.97	0	0.28	0.03

557 4.5. Soil water content (SWC)

558 From the comparison between AquaCrop simulations and in situ measurements of soil water
 559 content (SWC) (Fig. 9 and Table 10), for each crop type, we noted that AquaCrop simulated
 560 this variable very well, with R^2 values between 0.76 and 0.95 and RMSE values between 18.5
 561 mm and 32 mm. The best simulations were observed with oats. The MBE values indicated that
 562 the model simulations slightly underestimated the SWC observations for oats and faba beans
 563 and slightly overestimated them for wheat and barley. Despite these favourable results, we
 564 noted that the regression slope could be far from the 1:1 line for wheat. Additionally, we could
 565 not conclude on any possible trend to over- or underestimation according to the magnitude of
 566 in situ measurements. Indeed, the regression slopes were lower than one, apart from oats (1.04).
 567 For oats and barley, the *t* test provided *p* values larger than 5%. For wheat, the *t* test provided
 568 *p* value lower than 5%. For faba bean, the *t* test provided a *p* value lower than 5% for slope.

569



570

571 **Fig. 9.** Comparison between simulated and observed soil water content (SWC) on a crop type

572 basis. Each scatterplot corresponds to a crop type for several years and/or several plots.

573 Each dataset is indicated by a different marker and a different colour. Px, A, B, D relates to

574 plots and YYYY to years. The black line corresponds to the regression line, and the black

575 dashed line corresponds to the 1:1 line.

576 **Table 10.** Statistical indicators when comparing simulations against observations for soil wa-

577 ter content (SWC) on a crop type basis. n is the observation number. R^2 is the correlation co-

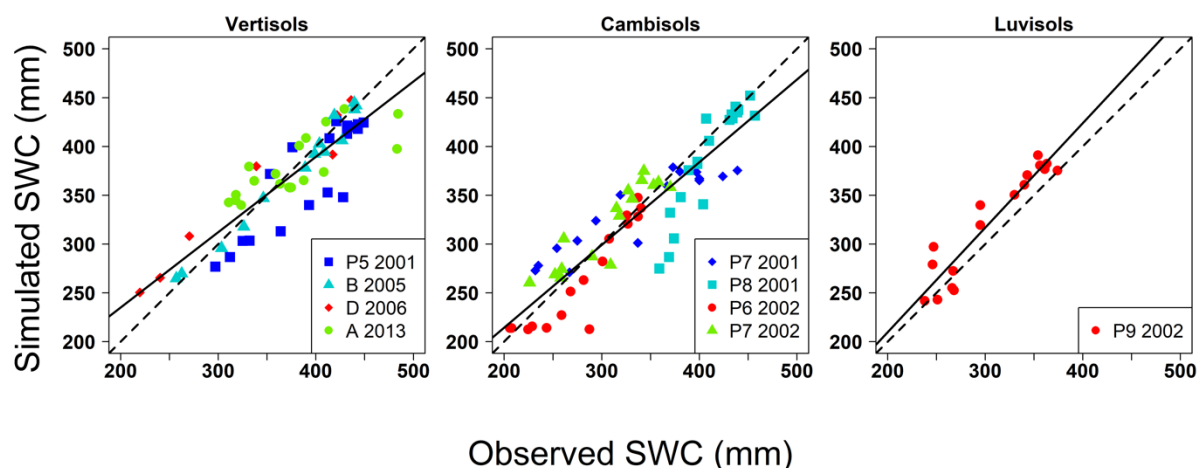
578 efficient. The t test corresponds to the p values of the Student's t test. The statistical indica-

579 tors RMSE, NRMSE and MBE are defined in Section 3.4.

Crop	Var	n	R^2 (-)	Offset (mm)		Slope (-)		RMSE (mm)	NRMSE (%)	MBE (mm)
				Value	t test	Value	t test			

Wheat	SWC	52	0.77	113.86	0	0.68	0	30.93	9	5.33
Oats		30	0.95	-21.70	0.14	1.04	0.33	18.51	6	-8.05
Barley		7	0.95	72.63	0.05	0.84	0.11	28.17	8	18.71
Faba		55	0.76	48.99	0.05	0.84	0.01	31.98	9	-11.71

580 The comparison between simulated and in situ measurements of SWC (Fig. 10 and Table 11),
581 for each soil class, showed that the model well simulated SWC for the 3 soil classes, with a
582 trend to underestimate observations for Vertisols and Cambisols and overestimate observations
583 for Luvisols. The R^2 values were above 0.79, with a relative variation of approximately 12%
584 across the three soil classes. The RMSE values ranged from 25 mm to 30 mm, and the regres-
585 sion slopes were lower than one, apart from Luvisols. For Luvisols, the t test provided p value
586 larger than 5%. For Vertisols and Cambisols, the t test provided p values lower than 5%.



588 **Fig. 10.** Comparison between simulated and observed soil water content (SWC) on a soil
589 class basis. Each scatterplot corresponds to a soil class for several plots, years and crops.
590 Each dataset is indicated by a different marker and a different colour. Px, A, B, D relates to
591 plots and YYYY to years. The black line corresponds to the regression line, and the black
592 dashed line corresponds to the 1:1 line.

594 **Table 11.** Statistical indicators when comparing simulations against observations for soil wa-
 595 ter content (SWC) on a soil class basis. n is the observation number. R^2 is the correlation co-
 596 efficient. The t test corresponds to the p values of the Student's t test. The statistical indica-
 597 tors RMSE, NRMSE and MBE are defined in Section 3.4.

Soil	Var	n	R^2 (-)	Offset (mm)		Slope (-)		RMSE (mm)	NRMSE (%)	MBE (mm)
				Value	t test	Value	t test			
Vertisols	SWC	59	0.79	80.77	0	0.77	0	28.41	8	-5.37
Cambisols		68	0.82	44.75	0.01	0.85	0	30.51	9	-6.69
Luvisols		17	0.89	-4.38	0.89	1.07	0.48	25.30	8	17.29

598 5. Discussion

599 5.1. Canopy cover (CC)

600 The large RMSE and NRMSE values on CC were ascribed to an overestimation of CC obser-
 601 vations by AquaCrop simulations throughout the senescence phase. This overestimation could
 602 result from the fact that the model disregarded the effect of high temperatures on crop func-
 603 tioning during the senescence phase (Andarzian et al., 2011). First, AquaCrop accounted for
 604 the effect of heat stress (low and high temperatures) on the pollination and harvest index only.
 605 Second, the early senescence we observed was not due to water stress: the seasonal courses of
 606 ET_a and ET_0 observed for wheat in 2013 in plot A (Fig. SP4) started to diverge as of DAS 140
 607 (19 Apr 2013), while senescence began at DAS 120 (30 Mar 2013). According to local farmers,
 608 early or sudden senescence of vegetation after heat waves has been observed in Kamech.
 609 Other studies reported overestimations of field observations by AquaCrop for CC at the end of
 610 the crop cycle for wheat in arid / semiarid climates, with lower magnitudes (Andarzian et al.,
 611 2011; Sghaier et al., 2014; Toumi et al., 2016). Beyond such differences during the senescence,
 612 the method used to convert LAI to CC for cereals might be an additional source of uncertainty,
 613 since the conversion was calibrated on hemispherical photos and applied on planimetric meas-
 614 urements, both observation types leading to physical differences (Jonckheere et al (2005).

615 5.2. Aboveground Biomass (AGB)

1
2
3 616 AquaCrop simulated AGB well, with an overestimation trend at the end of the crop cycle (e.g.,
4
5 617 faba bean, Fig. SP3). This could be ascribed to the overestimation of CC observations by Aq-
6
7
8 618 uaCrop simulations during the senescence phase in relation to a possible delay in senescence
9
10 619 by model simulations. For faba bean plot P5 in 2001, this could not be shown due to the lack
11
12 620 of CC measurements at the end of the crop cycle. However, Fig. SP2 indicates a recurrent
13
14
15 621 overestimation of CC observations by AquaCrop simulations at the end of the crop cycle for
16
17 622 different crop types and soil classes. Other studies have reported an overestimation of AGB
18
19
20 623 observations by AquaCrop simulations, either at the end of the crop cycle (Katerji et al., 2013;
21
22 624 Ahmadi et al., 2015; Sandhu and Irmak, 2019) or during the growth phase (Sghaier et al., 2014).

25 625 5.3. Actual evapotranspiration (ET_a)

26
27
28 626 AquaCrop showed acceptable performance in simulating ET_a for wheat and oats, with a trend
29
30
31 627 to slightly overestimate observations. The overestimation of ET_a from DAS 130 (9 April 2013)
32
33 628 for wheat and DAS 140 (3 May 2005) for oats could be related to the overestimation of CC
34
35
36 629 observations during the senescence. Masasi et al. (2019) reported a similar trend for sorghum
37
38 630 in a semiarid climate, and they suspected large atmospheric evaporative demand and poor char-
39
40
41 631 acterizations of soil hydrodynamic parameters. Despite this overestimation in ET_a, AquaCrop
42
43 632 well reproduced the divergence between ET_a and ET₀ courses at the end of the crop cycle.

44
45
46 633 The differences between simulated and observed ET_a values could also be due to (1) the eddy
47
48 634 covariance measurements that tend to underestimate ET_a (Boudhina et al., 2019; Leuning et
49
50
51 635 al., 2012), and (2) the reconstruction of missing ET_a data that induces uncertainties (Boudhina
52
53 636 et al., 2018; Zitouna-Chebbi et al., 2018). Besides, Katerji et al. (2013) recalled that the ET_a
54
55
56 637 calculation method in AquaCrop has been subject to several criticisms, especially when applied
57
58 638 in semiarid Mediterranean regions (Katerji and Rana, 2006; Lovelli et al., 2007). A first source
59
60
61
62

639 of error is assuming a constant surface resistance, since several studies in semiarid and arid
640 regions have shown that it leads to underestimating ET_0 compared to lysimeter measurements
641 (Katerji and Rana 2006). A second source of error is using the default value proposed by Allen
642 et al. (1998) for cultural coefficient K_c , since several works reported differences up to 40%
643 between this value and those observed in situ (Katerji and Rana 2006).

644 In contrast to the present study, previous works reported an underestimation for ET_a by Aqua-
645 Crop for maize and tomato (Katerji et al., 2013) and for wheat (Toumi et al., 2016) in a Medi-
646 terranean climate. No explanation could be found for this contradiction. For two calibration
647 plots, Toumi et al. (2016) reported RMSE values of 0.47 mm day^{-1} and 0.69 mm day^{-1} , which
648 were similar to the RMSE value found in the current study for wheat in 2013 in plot A.

649 **5.4. Runoff (R)**

650 For wheat in plot P7 in 2001, wheat in plot P9 in 2002, and oat in plot P6 in 2002, AquaCrop
651 simulated significant runoff values on DAS 19 (3 Dec 2000), DAS 2 (13 Dec 2001), and DAS
652 12 (11 Dec 2001), respectively. However, we could not evaluate AquaCrop simulations before
653 the second half of December, due to the lack of in situ measurements. However, it was possible
654 to verify the potential occurrence of runoff. According to Mekki (2003), rainfall greater than
655 20 mm day^{-1} is likely to generate runoff, regardless of surface conditions. Thus, the rainfall
656 recorded on DAS 19 for plot P7 in 2001, DAS 2 for plot P9 in 2002, and DAS 12 for plot P6
657 in 2002 were equal to 40 mm, 20 mm, and 28 mm, respectively (data not shown), which could
658 have produced runoff. This was also consistent with the slight increase of outlet lake level in
659 early December (compared to mid-November, data not shown). Overall, the runoff simulations
660 by AquaCrop early in the crop cycle were consistent with observations and expert knowledge.
661 For wheat in plot P9 in 2002 (DAS 10, 21 Dec 2001), wheat in plot A in 2013 (DAS 9, 09 Dec
662 2012), and oats in plot P6 in 2002 (DAS 20, 19 Dec 2001), we noted large values of model-

663 simulated runoff early in the crop cycle, but we did not observe coincident runoff events from
664 field observations. We observed the same difference between simulated and unobserved peak
665 runoff at the end of the crop cycle, for wheat in 2013 in plot A and for oats in 2002 in plot P6.
666 This could be explained by the presence of shrinkage cracks, which are known to generate
667 preferential infiltration at the expense of runoff (Inoubli et al., 2017).

668 Wolka et al (2021) reported one of the few assessments on the ability of AquaCrop to simulate
669 runoff. They noted that AquaCrop simulated runoff with RMSE values ranging from 9.8 mm
670 to 61.5 mm. However, it was difficult to compare these results with ours, because of larger
671 rainfall and runoff accumulations for Wolka et al. (2021).

672 **5.5. Soil water content (SWC)**

673 AquaCrop showed good performance in simulating soil water content. For oats, the underesti-
674 mation of SWC observations was ascribed to the overestimations of ET_a and runoff. The dif-
675 ferences between simulations and observations could be due to (1) inaccurate soil moisture
676 initialisations, (2) poor characterizations of soil hydrodynamic properties (HWP and HFC) and
677 (3) inadequate AquaCrop formalisms when simulating water fluxes (ET_a , runoff, drainage).
678 Additionally, disregarding capillary rise was not critical because most plots were located at
679 slope tops and therefore relatively far from possible shallow aquifers. Overall, the errors in
680 SWC simulations were ascribed to the characterization of soil hydrodynamic properties (HWP
681 and HFC), given the accuracies of AquaCrop simulations for water fluxes and crop variables.

682 Previous studies reported overestimations of SWC observations by AquaCrop simulations, no-
683 tably for wheat (Andarzian et al., 2011), maize (Nyakudya and Stroosnijder, 2014) and barley
684 (El Mokh et al., 2017). These overestimations were often noticed during dry periods, which
685 can be explained by constraints on SWC, since the latter cannot drop below HWP.

686 **5.6. Analysis by crop type and soil class**

687 When dealing with AquaCrop performance according to crop type, AquaCrop could be used
688 for predicting crop growth and biomass production. Oat crops could be used as animal fodder,
689 which is a common practice within Kamech and the surrounding region, with subsequent graz-
690 ing and cutting operations throughout the crop cycle. However, AquaCrop does not account
691 for the dynamics of the crop canopy induced by such agricultural practices. Nyathi et al (2018)
692 tried to parameterize this practice for leafy vegetables, by performing independent simulations
693 for any crop and assuming that the initial canopy cover (CC0) was reset according to the re-
694 maining canopy cover (from 1 to 2%) after each harvest.

695 When dealing with AquaCrop performance according to soil class, the analysis of model sim-
696 ulations permitted us to draw partial conclusions only. The analysis of the model outputs for
697 the AGB and SWC showed an acceptable performance in simulating these two variables across
698 all soil classes. For runoff and CC, the best results were observed with Vertisols and Cambisols,
699 respectively. For ET_a , for which we had measurements on Vertisols only, no conclusion can be
700 drawn regarding AquaCrop performance according to soil class.

701 When dealing with linear regressions on validation for both crop types and soil classes, the
702 t test provided p values larger than 5% for most cases (e.g., AGB, CC, SWC), which indicated
703 that AquaCrop performances could be considered satisfactory. For some crop/soil combina-
704 tions, the t test provided p values lower than 5% (e.g., ET_a , R, SWC), although the offset re-
705 mained relatively low (e.g., ET_a and SWC offset for oats and Cambisols, respectively).

706 **5.7. Main outcomes**

707 To our knowledge, the present work is the first study using AquaCrop for faba bean and oats
708 in a semiarid Mediterranean climate. According to the results we obtained, AquaCrop can ac-
709 ceptably simulate the functioning of these two crops by using crop parameters available in the

1
2 710 literature. Additionally, AquaCrop simulations are acceptable for various combinations of soils
3 711 and crops across contrasted hydroclimatic years.
4

5 712 Although there were gaps in database on which the current study relied, it was rich enough to
6
7 713 draw several lessons. According to the results we obtained, the model performance was closely
8
9 714 related to the formalism used for simulations. AquaCrop showed good performance in simu-
10
11 715 lating biomass and soil water content for all crops, on the basis of parameterizations and forcing
12
13 716 (1) that were as adequate as possible for the crops and soils to be studied, and (2) that were in
14
15 717 line with literature recommendations. The performance of the model was moderate for the sim-
16
17 718 ulation of CC, with a possible delay in senescence for most of the crops we addressed. The
18
19 719 model showed acceptable performance in simulating ET_a , although it was delicate to conclude
20
21 720 according to the dataset size (2 years - plots).
22
23
24
25
26

27 721 Runoff was poorly simulated at both the beginning and end of the crop cycle because of shrink-
28
29 722 age cracks for clay soils. Soil cracking is a complex phenomenon that is very difficult to include
30
31 723 in numerical modelling, especially in simplified models. Runoff simulations were acceptable
32
33 724 for the other stages of the crop cycle when the cracks were closed. Despite this, the simulations
34
35 725 were acceptable to simulate the dynamics of soil water content and crop variables (AGB), as
36
37 726 shown in Figs. 4-5-9-10 and Tabs 5-6-10-11, which was ascribed to the moderate influence of
38
39 727 runoff on the soil water balance. However, in the perspective of agro-hydrological studies that
40
41 728 require the consideration of lateral fluxes between the different components of the cultivated
42
43 729 landscape (Van Loo and Verstraeten, 2021), the runoff modelling by AquaCrop was no longer
44
45 730 acceptable for our study site, and it will be necessary to consider a more realistic runoff-infil-
46
47
48
49
50 731 tration partitioning model.
51
52
53

54 732 **6. Conclusion**

55
56
57
58
59
60
61
62

1 733 For some soil/crop combinations that have been little studied to date, AquaCrop can acceptably
2 734 simulate their functioning in terms of vegetation growth and water consumption, as well as in
3
4 735 terms of soil water balance, by using parameters available in the literature. Additionally, Aq-
5
6
7 736 uaCrop can simultaneously simulate several variables in an acceptable manner, namely, above-
8
9
10 737 ground biomass, evapotranspiration, and soil water content. We highlight some limitations of
11
12 738 AquaCrop in terms of vegetation cover and runoff in relation to delayed senescence and disre-
13
14
15 739 gard of swelling soils, respectively.

16
17 740 The results of the current study are in good agreement with those reported in the literature,
18
19
20 741 knowing that the previous studies mainly addressed flat terrains. Our study also showed that
21
22 742 AquaCrop was able to acceptably simulate crop dynamics and water fluxes for contrasted hy-
23
24
25 743 droclimatic years, with a slight dependence on soil class and a significant dependence on crop
26
27 744 type, including large differences from one variable to another.

28
29
30 745 Our results open the path for further use of AquaCrop in the Mediterranean context, on which
31
32 746 we focused, with forthcoming efforts on water availability and water productivity in relation
33
34
35 747 to plot hydrological connectivities within hilly terrains.

36 37 38 748 **Acknowledgements**

39
40
41 749 The first author benefited from funding provided by the Tunisian Ministry of Higher Education
42
43 750 and Scientific Research (MESRS) and the French National Research Institute for Sustainable
44
45
46 751 Development (IRD) to carry out her Ph.D. research. The current study is part of the ALTOS
47
48 752 project in the framework of the PRIMA program, with financial contributions from France and
49
50
51 753 Tunisia. The authors would like to thank (1) the Environmental Research Observatory OMERE
52
53 754 (<http://www.obs-omere.org>), which policy drives the availability of the data used in the current
54
55
56 755 study, and Damien Raclot, (2) Guillaume Coulouma (INRAE/UMR LISAH) for the help and
57
58
59
60
61
62
63
64
65

1 756 expertise provided in soil science, and (3) Marie Weiss (INRAE/UMR EMMAH) for the ex-
2 757 changes about CAN-EYE software.
3
4

5 **758 References**
6
7

8 759 Abrha, B., Delbecque, N., Raes, D., Tsegay, A., Todorovic, M., Heng, L., Vanutrecht, E.,
9

10 760 Geerts, S., Garcia-Vila, M., Deckers, S., 2012. Sowing strategies for barley
11

12 761 (HORDEUM VULGARE L.) based on modelled yield response to water with AQUA-
13

14 762 CROP. *Experimental Agriculture* 48, 252–271.
15
16

17
18 763 Ahmadi, S.H., Mosallaeepour, E., Kamgar-Haghighi, A.A., Sepaskhah, A.R., 2015. Modeling
19

20 764 Maize Yield and Soil Water Content with AquaCrop Under Full and Deficit Irrigation
21

22 765 Managements. *Water Resource Management* 29, 2837–2853.
23
24

25
26 766 Alaya, I., Masmoudi, M.M., Jacob, F., Ben Mechlia, N., 2019. Up-scaling of crop productivity
27

28 767 estimations using the AquaCrop model and GIS-based operations. *Arabian Journal of*
29

30 768 *Geosciences* 12, 419.
31
32

33
34 769 Allen, R.G., PEREIRA, L.S., RAES, D., SMITH, M. (Eds.), 1998. Crop evapotranspiration:
35

36 770 guidelines for computing crop water requirements, reprogaphy. ed, FAO irrigation and
37

38 771 drainage paper. Food and Agriculture Organization of the United Nations, Rome.
39
40

41
42 772 Andarzian, B., Bannayan, M., Steduto, P., Mazraeh, H., Barati, M.E., Barati, M.A., Rahnama,
43

44 773 A., 2011. Validation and testing of the AquaCrop model under full and deficit irrigated
45

46 774 wheat production in Iran. *Agricultural Water Management* 100, 1–8.
47
48

49
50 775 Araya, A., Habtu, S., Hadgu, K.M., Kebede, A., Dejene, T., 2010. Test of AquaCrop model in
51

52 776 simulating biomass and yield of water deficient and irrigated barley (*Hordeum vulgare*).
53

54 777 *Agricultural Water Management* 97, 1838–1846.
55
56

57
58 778 Bhattacharya, A., 2019. Chapter 3 - Water-Use Efficiency Under Changing Climatic Condi-
59

60 779 tions, *Changing Climate and Resource Use Efficiency in Plants* (A. Bhattacharya, Ed),
61
62

- 780 Academic Press, Pages 111-180, ISBN 9780128162095.
- 781 Besbes, B., Fournaraki, C., Tavolaro, F.M., Koutsovoulou, K., Leroy, G., Hoffmann, I., 2016.
782 Chapitre 6 - Diversité des ressources végétales et animales. Presses de Sciences Po.
- 783 Bird, D.N., Benabdallah, S., Gouda, N., Hummel, F., Koeberl, J., La Jeunesse, I., Meyer, S.,
784 Pretenthaler, F., Soddu, A., Woess-Gallasch, S., 2016. Modelling climate change im-
785 pacts on and adaptation strategies for agriculture in Sardinia and Tunisia using Aqua-
786 Crop and value-at-risk. *Science of The Total Environment*, Special Issue on Climate
787 Change, Water and Security in the Mediterranean 543, 1019–1027.
- 788 Boudhina, N., Masmoudi, M.M., Alaya, I., Jacob, F., Ben Mechlia, N., 2019. Use of AquaCrop
789 model for estimating crop evapotranspiration and biomass production in hilly topogra-
790 phy. *Arabian Journal of Geosciences* 12, 259.
- 791 Boudhina, N., Masmoudi, M.M., Ben Mechlia, N., Zitouna, R., Mekki, I., Prévot, L., Jacob, F.,
792 2017a. Evapotranspiration of Wheat in a Hilly Topography: Results from Measure-
793 ments Using a Set of Eddy Covariance Stations, in: Ouessar, M., Gabriels, D., Tsu-
794 nekawa, A., Evett, S. (Eds.), *Water and Land Security in Drylands: Response to Climate*
795 *Change*. Springer International Publishing, Cham, pp. 67–76.
- 796 Boudhina, N., Masmoudi, M.M., Jacob, F., Prévot, L., Zitouna, R., Mekki, I., Kallel, A., Ksibi,
797 M., Ben Dhia, H., Khélifi, N., 2017b. Measuring Crop Evapotranspiration Over Hilly
798 Areas, in: *Recent Advances in Environmental Science from the Euro-Mediterranean*
799 *and Surrounding Regions*. Springer International Publishing, pp. 909–911.
- 800 Boudhina, N., Zitouna-Chebbi, R., Mekki, I., Jacob, F., Ben Mechlia, N., Masmoudi, M., Pré-
801 vot, L., 2018. Evaluating four gap-filling methods for eddy covariance measurements
802 of evapotranspiration over hilly crop fields. *Geoscientific Instrumentation, Methods*
803 *and Data Systems* 7, 151–167.

- 804 Brisson, N., Gary, C., Justes, E., Roche, R., Mary, B., Ripoche, D., Zimmer, D., Sierra, J.,
1
2 805 Bertuzzi, P., Burger, P., Bussi re, F., Cabidoche, Y.M., Cellier, P., Debaeke, P.,
3
4 806 Gaudill re, J.P., H nault, C., Maraux, F., Seguin, B., Sinoquet, H., 2003. An overview
5
6
7 807 of the crop model STICS. *European Journal of Agronomy, Modelling Cropping Sys-*
8
9
10 808 *tems: Science, Software and Applications* 18, 309–332.
- 11
12 809 Brun, M., Blanc, P., Otto, H., 2016. *Chapitre 1 - Perspective globale des ressources naturelles.*
13
14
15 810 *Presses de Sciences Po.*
- 16
17
18 811 Cassel, D.K., Nielsen, D.R., 1986. Field Capacity and Available Water Capacity, in: Klute, A.
19
20 812 (Ed.), *SSSA Book Series. Soil Science Society of America, American Society of*
21
22
23 813 *Agronomy, Madison, WI, USA, pp. 901–926.*
- 24
25
26 814 Constantin, J., Willaume, M., Murgue, C., Lacroix, B., Therond, O., 2015. The soil-crop mod-
27
28 815 els STICS and AqYield predict yield and soil water content for irrigated crops equally
29
30
31 816 well with limited data. *Agricultural and Forest Meteorology* 206, 55–68.
- 32
33
34 817 Cusicanqui, J., Dillen, K., Garcia, M., Geerts, S., Raes, D., Mathijs, E., 2013. Economic as-
35
36 818 sessment at farm level of the implementation of deficit irrigation for quinoa production
37
38
39 819 in the Southern Bolivian Altiplano. *Spanish Journal of Agricultural Research* 11, 894.
- 40
41
42 820 de Wit, A., Boogaard, H., Fumagalli, D., Janssen, S., Knapen, R., van Kraalingen, D., Supit, I.,
43
44 821 van der Wijngaart, R., van Diepen, K., 2019. 25 years of the WOFOST cropping sys-
45
46 822 tems model. *Agricultural Systems* 168, 154–167.
- 47
48
49 823 Deb, P., Shrestha, S., Babel, M.S., 2015. Forecasting climate change impacts and evaluation of
50
51
52 824 adaptation options for maize cropping in the hilly terrain of Himalayas: Sikkim, India.
53
54 825 *Theoretical and Applied Climatology* 121, 649–667.
- 55
56
57 826 El Mokh, F., Vila-Garcia, Nagaz, K., Masmoudi, M.M., Ben Mechlia, N., Fereres, E., 2017.
58
59
60
61
62
63
64
65

- 827 Calibration of AquaCrop Salinity Stress Parameters for Barley Under Different Irriga-
1
2 828 tion Regimes in a Dry Environment, in: *Water and Land Security in Drylands; Re-*
3
4
5 829 sponse to Climate Change.
- 6
7
8 830 Er-Raki, S., Bouras, E., Rodriguez, J.C., Watts, C.J., Lizarraga-Celaya, C., Chehbouni, A.,
9
10 831 2021. Parameterization of the AquaCrop model for simulating table grapes growth and
11
12 832 water productivity in an arid region of Mexico. *Agricultural Water Management* 245,
13
14 833 106585.
- 15
16
17
18 834 García-López, J., Lorite, I., García-Ruiz, R., Domínguez, J., 2014. Evaluation of three simula-
19
20 835 tion approaches for assessing yield of rainfed sunflower in a Mediterranean environ-
21
22 836 ment for climate change impact modelling. *Climatic Change* 124, 147–162.
- 23
24
25
26 837 García-Vila, M., Fereres, E., 2012. Combining the simulation crop model AquaCrop with an
27
28 838 economic model for the optimization of irrigation management at farm level. *European*
29
30 839 *Journal of Agronomy* 36, 21–31.
- 31
32
33
34 840 Geerts, S., Raes, D., Garcia, M., Taboada, C., Miranda, R., Cusicanqui, J., Mhizha, T., Vacher,
35
36 841 J., 2009. Modeling the potential for closing quinoa yield gaps under varying water
37
38 842 availability in the Bolivian Altiplano. *Agricultural Water Management* 96, 1652–1658.
- 39
40
41 843 Han, C., Zhang, B., Chen, H., Wei, Z., Liu, Y., 2019. Spatially distributed crop model based
42
43 844 on remote sensing. *Agricultural Water Management* 218, 165–173.
- 44
45
46
47 845 Inoubli, N., 2016. Ruissellement et érosion hydrique en milieu méditerranéen verticale : ap-
48
49 846 proche expérimentale et modélisation (thèse de doctorat). Montpellier SupAgro ; Insti-
50
51 847 tut national agronomique de Tunisie.
- 52
53
54
55 848 Inoubli, N., Raclot, D., Mekki, I., Moussa, R., Le Bissonais, Y., 2017. A Spatiotemporal Mul-
56
57 849 tiscala Analysis of Runoff and Erosion in a Mediterranean Marly Catchment. *Vadose*
58
59 850 *Zone Journal* 16:1-12.
- 60
61
62
63
64
65

- 1
2
3
4
5
6
7
8
9
10
11
12
13
14
15
16
17
18
19
20
21
22
23
24
25
26
27
28
29
30
31
32
33
34
35
36
37
38
39
40
41
42
43
44
45
46
47
48
49
50
51
52
53
54
55
56
57
58
59
60
61
62
63
64
65
- 851 International Assessment of Agricultural Knowledge, Science and Technology for Develop-
852 ment Executive Summary of the Synthesis Report, 2008. International Assessment of
853 Agricultural Knowledge, Science and Technology for Development.
- 854 Jacob, F., Olivoso, A., Weiss, M., Baret, F., Hautecoeur, O., 2002. Mapping short-wave albedo
855 of agricultural surfaces using airborne POLDER data. *Remote Sensing of Environment*
856 80, 36–46.
- 857 Jamieson, P.D., Porter, J.R., Wilson, D.R., 1991. A test of the computer simulation model
858 ARCWHEAT1 on wheat crops grown in New Zealand. *Field Crops Research* 27, 337–
859 350.
- 860 Jonckheere, I., Fleck, S., Nackaerts, K., Muys, B., Coppin, P., Weiss, M., & Baret, F., 2004.
861 Review of methods for in situ leaf area index determination: Part I. Theories, sensors
862 and hemispherical photography. *Agricultural and Forest Meteorology*, 121(1-2), 19-35.
- 863 Jones, J.W., Antle, J.M., Basso, B., Boote, K.J., Conant, R.T., Foster, I., Godfray, H.C.J., Her-
864 rero, M., Howitt, R.E., Janssen, S., Keating, B.A., Munoz-Carpena, R., Porter, C.H.,
865 Rosenzweig, C., Wheeler, T.R., 2017. Brief history of agricultural systems modeling.
866 *Agricultural Systems* 155, 240–254.
- 867 Jones, J.W., Hoogenboom, G., Porter, C.H., Boote, K.J., Batchelor, W.D., Hunt, L.A., Wilkens,
868 P.W., Singh, U., Gijsman, A.J., Ritchie, J.T., 2003. The DSSAT cropping system
869 model. *European Journal of Agronomy, Modelling Cropping Systems: Science, Soft-*
870 *ware and Applications* 18, 235–265.
- 871 Kanda, E., Mabhaudhi, T., Senzanje, A., 2018. Coupling hydrological and crop models for
872 improved agricultural water management – A review. *Bulgarian Journal of Agricultural*
873 *Science* 23, 380.
- 874 Katerji, N., Campi, P., Mastrorilli, M., 2013. Productivity, evapotranspiration, and water use

- 875 efficiency of corn and tomato crops simulated by AquaCrop under contrasting water
1
2 876 stress conditions in the Mediterranean region. *Agricultural Water Management* 130,
3
4 877 14–26.
5
6
7 878 Katerji, N., Rana, G., 2006. Modelling evapotranspiration of six irrigated crops under Mediter-
8
9 ranean climate conditions. *Agricultural and Forest Meteorology* 138, 142–155.
10 879
11
12 880 Keating, B.A., Carberry, P.S., Hammer, G.L., Probert, M.E., Robertson, M.J., Holzworth, D.,
13
14 881 Huth, N.I., Hargreaves, J.N.G., Meinke, H., Hochman, Z., McLean, G., Verburg, K.,
15
16 882 Snow, V., Dimes, J.P., Silburn, M., Wang, E., Brown, S., Bristow, K.L., Asseng, S.,
17
18 883 Chapman, S., McCown, R.L., Freebairn, D.M., Smith, C.J., 2003. An overview of
19
20 884 APSIM, a model designed for farming systems simulation. *European Journal of Agron-*
21
22 omy, *Modelling Cropping Systems: Science, Software and Applications* 18, 267–288.
23 885
24
25 886 Kustas, W.P., Humes, K.S., Norman, J.M., Moran, M.S., 1996. Single- and Dual-Source Mod-
26
27 eling of Surface Energy Fluxes with Radiometric Surface Temperature. *Journal of Ap-*
28 887
29
30 888 *plied Meteorology and Climatology* 35, 110–121.
31
32
33 889 Leuning, R., van Gorsel, E., Massman, W.J., Isaac, P.R., 2012. Reflections on the surface en-
34
35 ergy imbalance problem. *Agricultural and Forest Meteorology* 156, 65–74.
36 890
37
38 891 Lovelli, S., Perniola, M., Ferrara, A., Di Tommaso, T., 2007. Yield response factor to water
39
40 (Ky) and water use efficiency of *Carthamus tinctorius* L. and *Solanum melongena* L.
41 892
42
43 893 *Agricultural Water Management* 92, 73–80.
44
45
46 894 Lu, Y., Chibarabada, T.P., McCabe, M.F., De Lannoy, G.J.M., Sheffield, J., 2021. Global sen-
47
48 sitivity analysis of crop yield and transpiration from the FAO-AquaCrop model for dry-
49 895
50
51 896 land environments. *Field Crops Research* 269, 108182.
52
53
54 897 Masasi, B., Taghvaeian, S., Gowda, P.H., Warren, J., Marek, G., 2019. Simulating Soil Water
55
56
57
58
59
60
61
62
63
64
65

- 898 Content, Evapotranspiration, and Yield of Variably Irrigated Grain Sorghum Using AquaCrop. *Journal of the American Water Resources Association* 55(4), 976–993.
- 899
- 900 Mekki, I., 2003. Analyse et modélisation de la variabilité des flux hydriques à l'échelle d'un
- 901 bassin versant cultivé alimentant un lac collinaire du domaine semi-aride méditerranéen
- 902 (Oued Kamech, Cap Bon, Tunisie) (Thèse de doctorat). Montpellier 2.
- 903 Mekki, I., Albergel, J., Ben Mechlia, N., Voltz, M., 2006. Assessment of overland flow varia-
- 904 tion and blue water production in a farmed semi-arid water harvesting catchment. *Physics and Chemistry of the Earth, Parts A/B/C* 31, 1048–1061.
- 905
- 906 Mekki, I., Bailly, J.S., Jacob, F., Chebbi, H., Ajmi, T., Blanca, Y., Zairi, A., Biarnès, A., 2018.
- 907 Impact of farmland fragmentation on rainfed crop allocation in Mediterranean land-
- 908 scapes: A case study of the Lebna watershed in Cap Bon, Tunisia. *Land Use Policy* 75,
- 909 772–783.
- 910 Mkhabela, M.S., Bullock, P.R., 2012. Performance of the FAO AquaCrop model for wheat
- 911 grain yield and soil moisture simulation in Western Canada. *Agricultural Water Man-*
- 912 *agement* 110, 16–24.
- 913 Molénat, J., Raclot, D., Zitouna, R., Andrieux, P., Coulouma, G., Feurer, D., Grünberger, O.,
- 914 Lamachère, J.M., Bailly, J.S., Belotti, J.L., Ben Azzez, K., Ben Mechlia, N., Ben
- 915 Younès Louati, M., Biarnès, A., Blanca, Y., Carrière, D., Chaabane, H., Dagès, C.,
- 916 Debabria, A., Dubreuil, A., Fabre, J.C., Fages, D., Floure, C., Garnier, F., Geniez, C.,
- 917 Gomez, C., Hamdi, R., Huttel, O., Jacob, F., Jenhaoui, Z., Lagacherie, P., Le Bis-
- 918 sonnais, Y., Louati, R., Louchart, X., Mekki, I., Moussa, R., Negro, S., Pépin, Y., Pré-
- 919 vot, L., Samouelian, A., Seidel, J.L., Trotoux, G., Troiano, S., Vinatier, F., Zante, P.,
- 920 Zrelli, J., Albergel, J., Voltz, M., 2018. OMERE: A Long-Term Observatory of Soil

- 921 and Water Resources, in Interaction with Agricultural and Land Management in Medi-
1
2 922 terranean Hilly Catchments. *Vadose Zone Journal* 17: 1-18 180086.
3
4
5 923 Montes, C., Lhomme, J.-P., Demarty, J., Prévot, L., Jacob, F., 2014. A three-source SVAT
6
7 924 modeling of evaporation: Application to the seasonal dynamics of a grassed vineyard.
8
9
10 925 *Agricultural and Forest Meteorology* 191, 64–80.
11
12
13 926 Moriasi, D.N., Arnold, J.G., Liew, M.W., Bingner, R.L., Harmel, R.D., Veith, T.L., 2007.
14
15 927 Model Evaluation Guidelines for Systematic Quantification of Accuracy in Watershed
16
17 928 Simulations. *Transactions of the ASABE* 50, 885–900.
18
19
20
21 929 Moriasi, D.N., Gitau, M.W., Pai, N., Daggupati, D., 2015. Hydrologic and Water Quality Mod-
22
23 930 els: Performance Measures and Evaluation Criteria. *Transactions of the ASABE* 58,
24
25 931 1763–1785.
26
27
28 932 Mubvuma, Michael.T., Ogola, J.B.O., Mhizha, T., 2021. AquaCrop model calibration and val-
29
30 933 idation for chickpea (*Cicer arietinum*) in Southern Africa. *Cogent Food & Agriculture*
31
32 934 7, 1898135.
33
34
35
36 935 Muluneh, A., 2020. Impact of climate change on soil water balance, maize production, and
37
38 936 potential adaptation measures in the Rift Valley drylands of Ethiopia. *Journal of Arid*
39
40 937 *Environments* 179, 104195.
41
42
43
44 938 Norouzi, M., Ayoubi, S., Jalalian, A., Khademi, H., Dehghani, A.A., 2010. Predicting rainfed
45
46 939 wheat quality and quantity by artificial neural network using terrain and soil character-
47
48 940 istics. *Acta Agriculturae Scandinavica, Section B — Soil & Plant Science* 60, 341–352.
49
50
51
52 941 Nouri, H., Stokvis, B., Chavoshi Borujeni, S., Galindo, A., Brugnach, M., Blatchford, M.L.,
53
54 942 Alaghmand, S., Hoekstra, A.Y., 2020. Reduce blue water scarcity and increase nutri-
55
56 943 tional and economic water productivity through changing the cropping pattern in a
57
58 944 catchment. *Journal of Hydrology* 588, 125086.
59
60
61
62
63
64
65

- 1
2
3
4
5
6
7
8
9
10
11
12
13
14
15
16
17
18
19
20
21
22
23
24
25
26
27
28
29
30
31
32
33
34
35
36
37
38
39
40
41
42
43
44
45
46
47
48
49
50
51
52
53
54
55
56
57
58
59
60
61
62
63
64
65
- 945 Nyakudya, I.W., Stroosnijder, L., 2014. Effect of rooting depth, plant density and planting date
946 on maize (*Zea mays* L.) yield and water use efficiency in semi-arid Zimbabwe: Model-
947 ling with AquaCrop. *Agricultural Water Management* 146, 280–296.
- 948 Nyathi, M.K., van Halsema, G.E., Annandale, J.G., Struik, P.C., 2018. Calibration and valida-
949 tion of the AquaCrop model for repeatedly harvested leafy vegetables grown under dif-
950 ferent irrigation regimes. *Agricultural Water Management* 208, 107–119.
- 951 Pereira, L.S., Paredes, P., Rodrigues, G.C., Neves, M., 2015. Modeling malt barley water use
952 and evapotranspiration partitioning in two contrasting rainfall years. *Assessing Aqua-
953 Crop and SIMDualKc models. Agricultural Water Management* 159, 239–254.
- 954 Qin, W., Chi, B., Oenema, O., 2013. Long-Term Monitoring of Rainfed Wheat Yield and Soil
955 Water at the Loess Plateau Reveals Low Water Use Efficiency. *PLOS ONE* 8, e78828.
- 956 Raes, D., Steduto, P., Hsiao, T.C., Fereres, E., 2009. AquaCrop -The FAO Crop Model to Sim-
957 ulate Yield Response to Water: II. Main Algorithms and Software Description. *Agron-
958 omy Journal* 101, 438–447.
- 959 Raoufi, R.S., Soufizadeh, S., 2020. Simulation of the impacts of climate change on phenology,
960 growth, and yield of various rice genotypes in humid sub-tropical environments using
961 AquaCrop-Rice. *International Journal of Biometeorology* 64, 1657–1673.
- 962 Rashid, M.A., Jabloun, M., Andersen, M.N., Zhang, X., Olesen, J.E., 2019. Climate change is
963 expected to increase yield and water use efficiency of wheat in the North China Plain.
964 *Agricultural Water Management* 222, 193–203.
- 965 Reichstein, M., Falge, E., Baldocchi, D., Papale, D., Aubinet, M., Berbigier, P., Bernhofer, C.,
966 Buchmann, N., Gilmanov, T., Granier, A., Grünwald, T., Havránková, K., Ilvesniemi,
967 H., Janous, D., Knohl, A., Laurila, T., Lohila, A., Loustau, D., Matteucci, G., Meyers,
968 T., Miglietta, F., Ourcival, J.-M., Pumpanen, J., Rambal, S., Rotenberg, E., Sanz, M.,

- 969 Tenhunen, J., Seufert, G., Vaccari, F., Vesala, T., Yakir, D., Valentini, R., 2005. On the
1 separation of net ecosystem exchange into assimilation and ecosystem respiration: re-
2 970 view and improved algorithm. *Global Change Biology* 11, 1424–1439.
3
4
5 971
6
7
8 972 Robinson, D.A., Campbell, C.S., Hopmans, J.W., Hornbuckle, B.K., Jones, S.B., Knight, R.,
9
10 973 Ogden, F., Selker, J., Wendroth, O., 2008. Soil Moisture Measurement for Ecological
11
12 974 and Hydrological Watershed-Scale Observatories: A Review. *Vadose Zone Journal* 7,
13
14 975 358–389.
15
16
17
18 976 Ruben, R., Pender, J., 2004. Rural diversity and heterogeneity in less-favoured areas: the quest
19
20 977 for policy targeting. *Food Policy* 29, 303–320.
21
22
23 978 Salman, M., García-Vila, M., Fereres, E., Raes, D., Steduto, P., 2021. The AquaCrop model–
24
25 979 Enhancing crop water productivity: Ten years of development, dissemination and im-
26
27 980 plementation 2009–2019 (Vol. 47). Food & Agriculture Organisation.
28
29
30
31 981 Sandhu, R., Irmak, S., 2019. Performance of AquaCrop model in simulating maize growth,
32
33 982 yield, and evapotranspiration under rainfed, limited and full irrigation. *Agricultural Wa-
34
35 983 ter Management* 223, 105687.
36
37
38
39 984 Sghaier, N., Masmoudi, M.M., Ben Mechlia, N., 2014. Paramétrage du modèle AquaCrop pour
40
41 985 la simulation de la culture du blé dur. *Revue des Régions Arides*, 35, 1351-1360.
42
43
44 986 Shrestha, S., Deb, P., Bui, T.T.T., 2016. Adaptation strategies for rice cultivation under climate
45
46 987 change in Central Vietnam. In: *Climate Change Impacts and Adaptation in Water Re-
47
48 988 sources and Water Use Sectors*. Springer Water. Springer, Cham 21, 15–37.
49
50
51
52 989 Silvestro, P.C., Pignatti, S., Pascucci, S., Yang, H., Li, Z., Guijun, Y., Huang, W., Casa, R.,
53
54 990 2017. Estimating Wheat Yield in China at the Field and District Scale from the Assim-
55
56 991 ilation of Satellite Data into the AquaCrop and Simple Algorithm for Yield (SAFY)
57
58 992 Models. *Remote Sensing* 9, 509.
59
60
61
62
63
64
65

- 1
2
3
4
5
6
7
8
9
10
11
12
13
14
15
16
17
18
19
20
21
22
23
24
25
26
27
28
29
30
31
32
33
34
35
36
37
38
39
40
41
42
43
44
45
46
47
48
49
50
51
52
53
54
55
56
57
58
59
60
61
62
63
64
65
- 993 Sreelash, K., Buis, S., Sekhar, M., Ruiz, L., Kumar Tomer, S., Guérif, M., 2017. Estimation of
994 available water capacity components of two-layered soils using crop model inversion:
995 Effect of crop type and water regime. *Journal of Hydrology* 546, 166–178.
- 996 Steduto, P., Hsiao, T.C., Raes, D., Fereres, E., 2009. AquaCrop-The FAO Crop Model to Sim-
997 ulate Yield Response to Water: I. Concepts and Underlying Principles. *Agronomy Jour-*
998 *nal* 101, 426–437.
- 999 Stöckle, C.O., Donatelli, M., Nelson, R., 2003. CropSyst, a cropping systems simulation model.
1000 *European Journal of Agronomy, Modelling Cropping Systems: Science, Software and*
1001 *Applications* 18, 289–307.
- 1002 Susha Lekshmi, S.U., Singh, D.N., Shojaei Baghini, M., 2014. A critical review of soil mois-
1003 ture measurement. *Measurement* 54, 92–105.
- 1004 Tanyeri-Abur, A., 2015. Food Security in the Southern Mediterranean/North Africa, in: Vas-
1005 tola, A. (Ed.), *The Sustainability of Agro-Food and Natural Resource Systems in the*
1006 *Mediterranean Basin*. Springer International Publishing, Cham, pp. 3–14.
- 1007 Todorovic, M., Albrizio, R., Zivotic, L., Saab, M.-T.A., Stöckle, C., Steduto, P., 2009. Assess-
1008 ment of AquaCrop, CropSyst, and WOFOST Models in the Simulation of Sunflower
1009 Growth under Different Water Regimes. *Agronomy Journal* 101, 509–521.
- 1010 Toumi, J., Er-Raki, S., Ezzahar, J., Khabba, S., Jarlan, L., Chehbouni, A., 2016. Performance
1011 assessment of AquaCrop model for estimating evapotranspiration, soil water content
1012 and grain yield of winter wheat in Tensift Al Haouz (Morocco): Application to irriga-
1013 tion management. *Agricultural Water Management* 163, 219–235.
- 1014 Tribouillois, H., Constantin, J., Willaume, M., Brut, A., Ceschia, E., Tallec, T., Beaudoin, N.,
1015 Therond, O., 2018. Predicting water balance of wheat and crop rotations with a simple
1016 model: AqYield. *Agricultural and Forest Meteorology* 262, 412–422.

- 1017 Van Loo, M., Verstraeten, G., 2021. A Spatially Explicit Crop Yield Model to Simulate Agri-
1
21018 cultural Productivity for Past Societies under Changing Environmental Conditions. Wa-
3
4
51019 ter 13, 2023.
6
7
81020 Vanuytrecht, E., Raes, D., Willems, P., 2014. Global sensitivity analysis of yield output from
9
101021 the water productivity model. *Environmental Modelling & Software* 51, 323–332.
11
12
131022 Walker, J.P., Willgoose, G.R., Kalma, J.D., 2004. In situ measurement of soil moisture: a com-
14
151023 parison of techniques. *Journal of Hydrology* 293, 85–99.
16
17
181024 Wani, S.P., Rockström, J., Oweis, T.Y., 2009. *Rainfed Agriculture: Unlocking the Potential*.
19
20
211025 CAB International, Wallingford, UK.
22
23
241026 Weiss, M., Jacob, F., Duveiller, G., 2020. Remote sensing for agricultural applications: A meta-
25
261027 review. *Remote Sensing of Environment*, 236, 111402.
27
28
291028 Williams, J.R., Jones, C.A., Dyke, P.T., 1984. A modelling approach to determining the rela-
30
31
321029 tionship between erosion and soil productivity [EPIC, Erosion-Productivity Impact Cal-
33
341030 culator, mathematical models]. *Transactions of the ASAE [American Society of Agri-
35
361031 cultural Engineers] (USA)*.
37
38
391032 Wolka, K., Biazin, B., Martinsen, V., Mulder, J., 2021. Soil and water conservation manage-
40
41
421033 ment on hill slopes in southwest Ethiopia. II. Modeling effects of soil bunds on surface
43
441034 runoff and maize yield using AquaCrop. *Journal of Environmental Management* 296,
45
46
471035 113187.
48
49
501036 Xing, H., Xu, X., Li, Z., Chen, Y., Feng, H., Yang, G., Chen, Z., 2017. Global sensitivity anal-
51
521037 ysis of the AquaCrop model for winter wheat under different water treatments based on
53
54
551038 the extended Fourier amplitude sensitivity test. *Journal of Integrative Agriculture* 16,
56
571039 2444–2458.
58
59
60
61
62
63
64
65

- 1040 Yang, J.M., Yang, J.Y., Liu, S., Hoogenboom, G., 2014. An evaluation of the statistical meth-
1
2 1041 ods for testing the performance of crop models with observed data. *Agricultural Sys-*
3
4
5 1042 tems 127, 81–89.
6
7
8 1043 Yuan, M., Zhang, L., Gou, F., Su, Z., Spiertz, J.H.J., van der Werf, W., 2013. Assessment of
9
10 1044 crop growth and water productivity for five C3 species in semi-arid Inner Mongolia.
11
12
13 1045 *Agricultural Water Management* 122, 28–38.
14
15
16 1046 Zeleke, K.T., 2019. AquaCrop Calibration and Validation for Faba Bean (*Vicia faba* L.) under
17
18 1047 Different Agronomic Managements. *Agronomy* 9, 320.
19
20
21 1048 Zitouna-Chebbi, R., Prévot, L., Chakhar, A., Marniche-Ben Abdallah, M., Jacob, F., 2018. Ob-
22
23 1049 serving Actual Evapotranspiration from Flux Tower Eddy Covariance Measurements
24
25
26 1050 within a Hilly Watershed: Case Study of the Kamech Site, Cap Bon Peninsula, Tunisia.
27
28 1051 *Atmosphere* 9, 68.
29
30
31 1052 Zitouna-Chebbi, R., Prévot, L., Jacob, F., Mougou, R., Voltz, M., 2012. Assessing the con-
32
33
34 1053 sistency of eddy covariance measurements under conditions of sloping topography
35
36 1054 within a hilly agricultural catchment. *Agricultural and Forest Meteorology* 164, 123–
37
38
39 1055 135.
40
41
42 1056 Zitouna-Chebbi, R., Prévot, L., Jacob, F., Voltz, M., 2015. Accounting for vegetation height
43
44 1057 and wind direction to correct eddy covariance measurements of energy fluxes over hilly
45
46 1058 crop fields. *Journal of Geophysical Research: Atmospheres* 120, 4920–4936.
47
48
49
50
51
52
53
54
55
56
57
58
59
60
61
62
63
64
65

1 **Supplementary materials - Section 1: materials and methods - soil parameters**

2 Different approaches are proposed in the literature to determine soil moisture at wilting point
3 (HWP) and at field capacity (HFC), including (1) pedotransfer functions (e.g., Saxton and
4 Rawls, 2006) based on the texture of different soil horizons, (2) direct laboratory measurements
5 from soil samples (Cassel and Nielsen, 1986) and (3) the agroclimatic method which determines
6 HFC and HWP from soil moisture time series throughout the crop growth cycle (Sreelash et al.,
7 2017).

8 According to expert knowledge about the soil conditions within our study site (Revaillot et al.,
9 2021), the pedotransfer functions are not suitable for the Kamech soils, since the latter are
10 typified by large instability due to poor silt structure. Therefore, we determine HWP and HFC
11 using the laboratory method and the agroclimatic method, and we compared the resulting
12 estimates in order to choose the most reliable ones.

13 For all plots, we had laboratory measurements of HFC and HWP carried out either on the plots
14 or on neighbouring plots, along with soil moisture data. For the agroclimatic method proposed
15 by Sreelash et al. (2017), HFC corresponds to the maximum soil moisture value without
16 considering measurements after rainfalls or irrigation events, and HWP corresponds to the 5th
17 percentile of the minimum soil moisture measured throughout the crop growth cycle. To
18 determine HFC and HWP by the agroclimatic method, we used all soil moisture data available
19 for each of the eight plots, beyond the datasets used for AquaCrop evaluation. This led to
20 include additional soil moisture data from 2002 on plot P5 and P8, from 2001 and plot P6 and
21 P9, and from 2006 on plot A. All the soil moisture measurements we considered were collected
22 using the same protocol described in the Section 3.3.6 of the article. For HFC, we assumed that
23 a rainfall accumulation lower than 10 mm does not have a large influence, and we therefore
24 excluded all measurements for which a rainfall accumulation larger than 10 mm was recorded
25 in the previous 48 hours. For HWP, we take the 5th percentile of the minimum value measured
26 throughout the crop growth cycle.

27 Table SP1 presents, for each plot, HWP and HFC estimates by laboratory measurements (Lab),
28 and by the agroclimatic method (AC), as well as the relative difference Δ calculated as:

$$29 \quad \Delta = \frac{AC - Lab}{Lab} \quad (\text{Equation SP1})$$

30 where AC (respectively Lab) represents the HWP or HFC estimates by the agroclimatic method
31 (respectively the laboratory method).

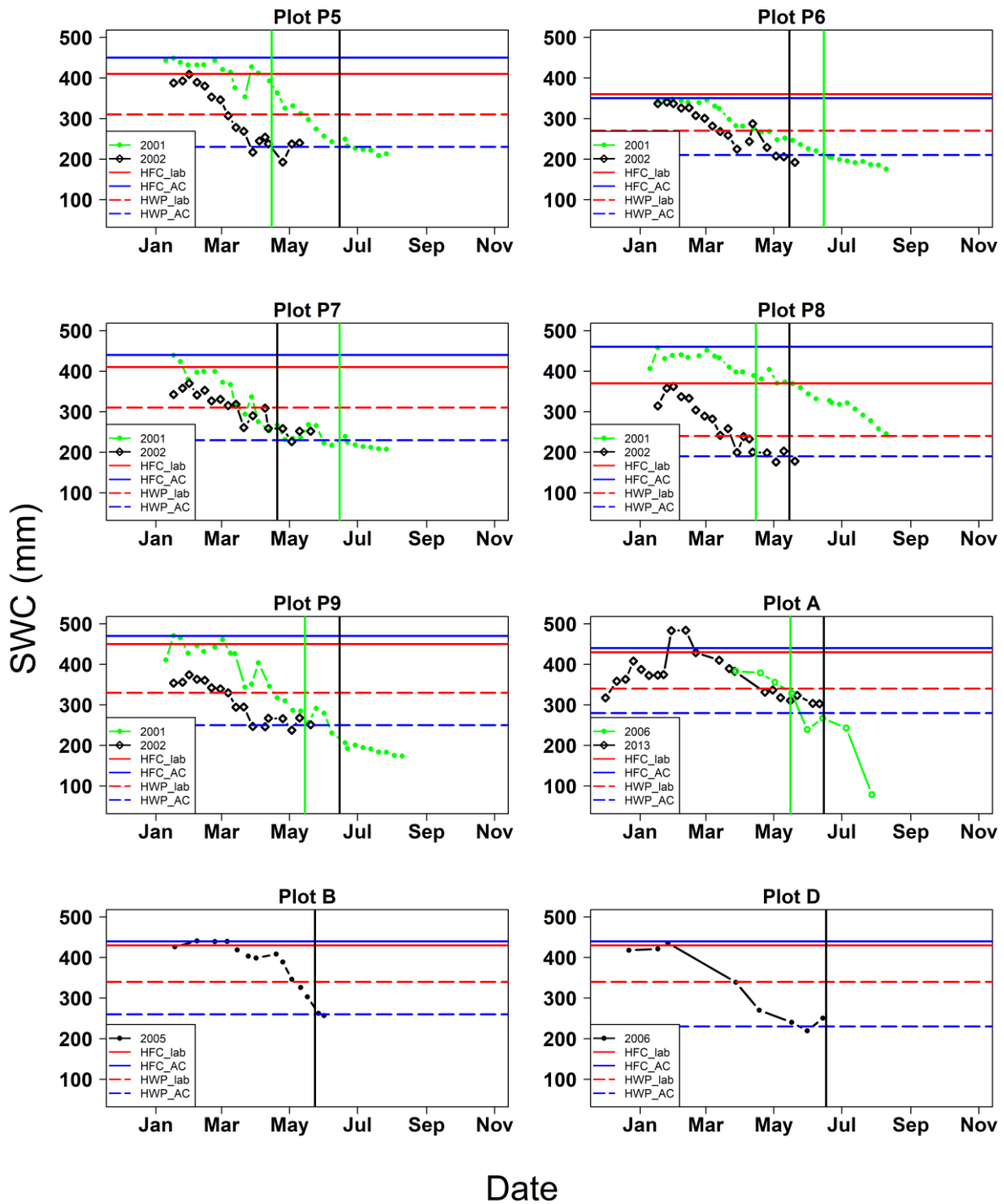
32 Table SP1 shows that HWP estimates from the agroclimatic method underestimated those from
 33 the laboratory method, with values of relative difference Δ between -26% and -18%, apart from
 34 plot D (32%). For HFC, the differences between the two methods were small, with values of
 35 relative difference Δ between -3% and 10%, apart from plot P8 (24%). In this case, HFC
 36 estimates from the agroclimatic method overestimated those from the laboratory method, apart
 37 from plot P6.

38 **Table SP1.** Comparison between soil moisture at wilting point (HWP) and soil moisture at
 39 field capacity (HFC) estimates by the laboratory measurements (Lab) and the agroclimatic
 40 method (AC) methods.

	HWP			HFC		
	AC (m ³ /m ³)	lab (m ³ /m ³)	Δ (%)	AC (m ³ /m ³)	lab (m ³ /m ³)	Δ (%)
P5	0.23	0.31	-26	0.45	0.41	10
P6	0.21	0.27	-22	0.35	0.36	-3
P7	0.23	0.31	-26	0.44	0.41	7
P8	0.19	0.24	-21	0.46	0.37	24
P9	0.25	0.33	-24	0.47	0.45	4
A	0.28	0.34	-18	0.44	0.43	2
B	0.26	0.34	-24	0.44	0.43	2
D	0.23	0.34	-32	0.44	0.43	2

41 Fig. SP1 displays the times series of soil moisture measurements, as well as the HFC and HWP
 42 estimates from (1) the laboratory measurements (HWP-lab and HFC-lab), and (2) the
 43 agroclimatic method (HWP-AC and HFC-AC) for each of all plots. Fig. SP1 shows that, apart
 44 from plot A, the soil moisture measurements before the harvest dates reach lower levels than
 45 the HWP estimates from the laboratory measurements.

46 As a result, we selected the estimates from the agroclimatic method for all plots apart from plot
 47 A. For plot A, the differences between estimates from both methods were very low
 48 (10% relative, comparable to measurement errors), and we selected the estimates from
 49 laboratory measurements that were collected in the framework of the OMERE observatory.



51

52 **Fig. SP1.** Time series of soil moisture data (dotted lines) for each of the eight plots. The
 53 horizontal lines indicate the soil moisture at wilting point (HWP) and soil moisture at field
 54 capacity (HFC) estimates from the laboratory measurements (Lab) (red lines) and
 55 agroclimatic method (AC) (blue lines) methods. The vertical lines indicate the harvest dates.

56

57 **Supplementary materials - Section 2: Materials and methods – Vegetation**

58 When dealing with growth cycle of cereals (wheat, barley, oats), we could use leaf area index
59 (LAI) measurements performed with planimeters. In order to validate the AquaCrop
60 simulations of canopy cover (CC), we used Equation SP2 to convert planimetry-based LAI data
61 into CC, considering that this equation had been used in many studies (Araya et al., 2010; Abrha
62 et al., 2012; Yuan et al., 2013; Pereira et al., 2015; Zeleke, 2019):

63
$$CC = 1 - e^{(-k \times LAI)} \quad \text{(Equation SP2)}$$

64 The coefficient k is an extinction coefficient related to the interception of light by crop canopy
65 cover (Jeuffroy and Ney, 1997; Pereira et al., 2015). It varies according to crop and variety.
66 Different values of k have been proposed in literature for a given crop. For example, the
67 proposed values for barley are k = 0.5 (Pereira et al., 2015), k = 0.48 (Belhouchette et al., 2008)
68 and k = 0.65 (Abrha et al., 2012). For wheat, (Jin et al., 2014) proposed a k value of 0.65.

69 To determine a k value that was suitable to our conditions, we used hemispherical photos that
70 permitted to simultaneously estimate LAI and CC. These photos were collected between 2018
71 and 2020 thanks to a camera equipped with a fisheye objective. Within each plot, between 10
72 and 15 photos were collected in a random manner. Table SP2 summarises the number of plots
73 and measurements available per crop.

74 **Table SP2.** Number of plots and hemispherical photos available for each crop, to be used for
75 determining the value of coefficient k in Equation SP2.

Crop	Years	Plot number	Measurements number
Wheat	2018 - 2019 - 2020	8	42
Barley	2019 - 2020	2	10
Oats	2020	1	4

76 The hemispherical photos were treated with the CAN-EYE software (Weiss et al., 2008) to
77 derive first gap fraction, and then LAI and CC. CAN-EYE permitted to distinguish two types
78 of LAI, namely (1) effective LAI that accounts for leaf aggregation, and (2) true LAI that
79 corresponds to actual leaf surface. The different LAI estimates proposed by CAN-EYE are
80 discussed in Weiss et al. (2008).

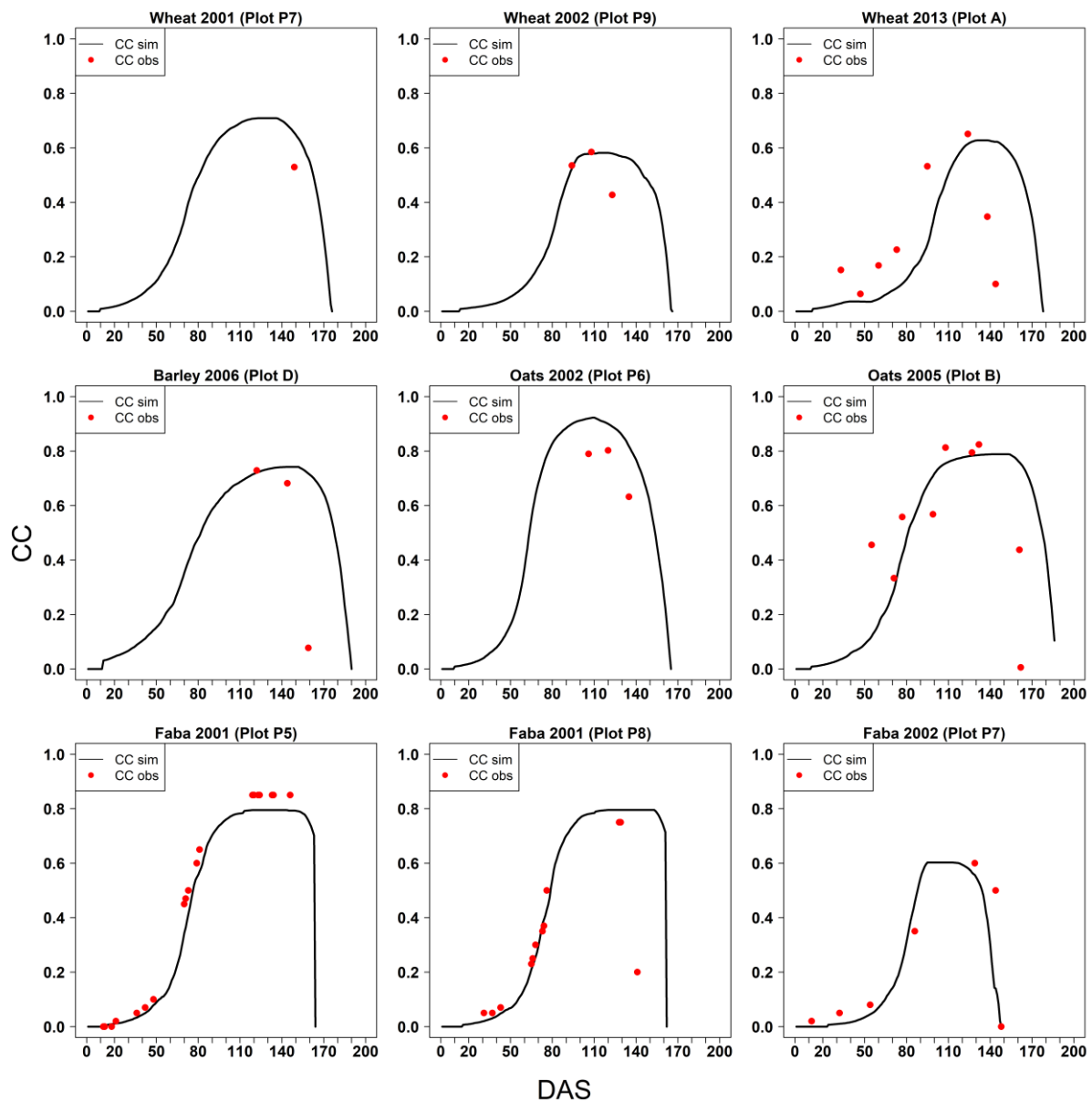
- 81 • On the one hand, planimetry is a direct and destructive technique for determining leaf area
82 index of any crop canopy. It permits the calculation of actual LAI from direct area
83 measurements.

- 84 • On the other hand, hemispherical photography is an indirect, non-destructive technique that
85 permits a significant spatiotemporal sampling of crop canopy within field and throughout
86 the crop growth cycle. It includes other plant green elements such as stems, which
87 corresponds to Plant Area Index (PAI) rather than LAI.
- 88 • The goal here was to convert planimetric measurements of LAI into CC estimates by using
89 Equation SP2. When estimating LAI from hemispherical photos, it was necessary to select
90 the CAN-EYE method that provided LAI estimates as close as possible to the planimetric
91 method. According to Weiss et al (2008), the true LAI calculated by CAN-EYE is the
92 closest to the planimetric LAI, although the relationship between true LAI measured by
93 CAN-EYE and planimetric LAI depends on crop and phenological stage (Demarez et al.,
94 2008; Fang et al., 2018). Therefore, we choose true LAI for equation SP2.

95 For the present study, we decided to set a single k value for cereals (wheat, barley and oats),
96 equal to 0.57 ($R^2 = 0.95$; $RMSE = 0.05$). Indeed, the coefficient of variation between the
97 different k values across cereal crops was about 15%, thus comparable to the measurement error
98 (Weiss et al., 2008). Moreover, the three cereal crops we considered were straw cereals with
99 similar leaf geometry that induces similar radiative transfer processes within the canopy.

100

102

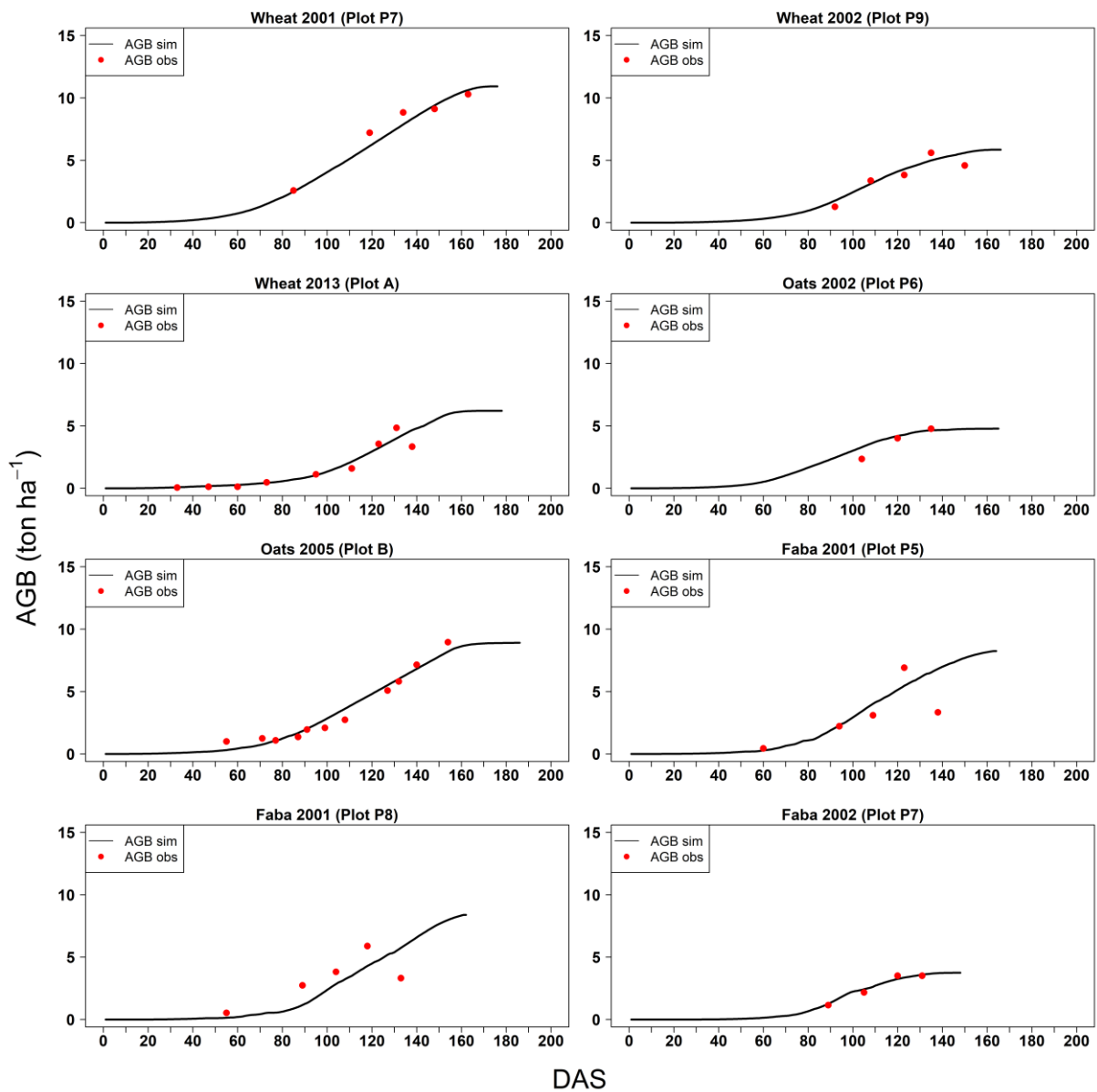


103

104 **Fig. SP2.** Temporal evolution of canopy cover (CC) for each dataset when available. The red
 105 points correspond to the ground-based observations, and the black curves correspond to the
 106 AquaCrop simulations. DAS stands for Day after Sowing.

107

109



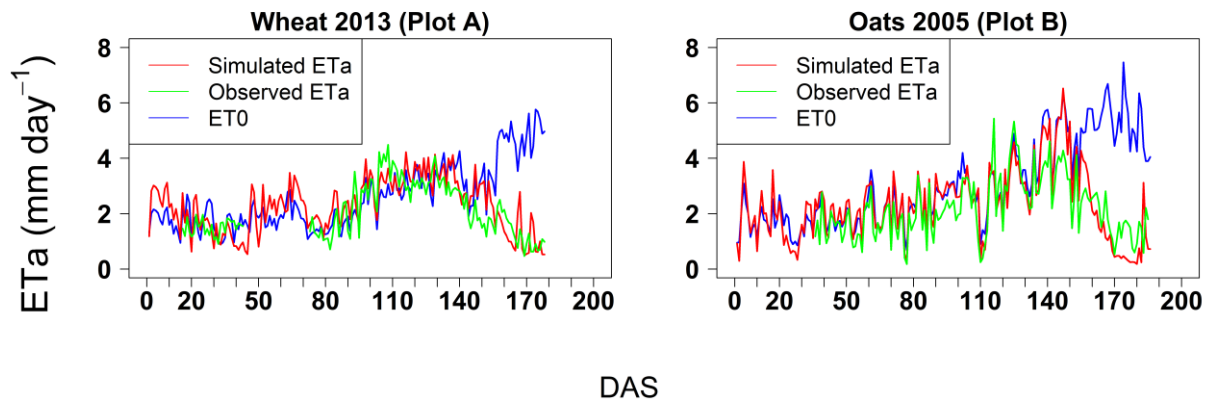
110

111 **Fig. SP3.** Temporal evolution of Aboveground biomass (AGB) for each dataset when
 112 available. The red points correspond to observations and the black curve corresponds to
 113 AquaCrop simulations. DAS stands for Day after Sowing.

114

115 **Supplementary materials - Section 5. Results - actual evapotranspiration (ETa)**

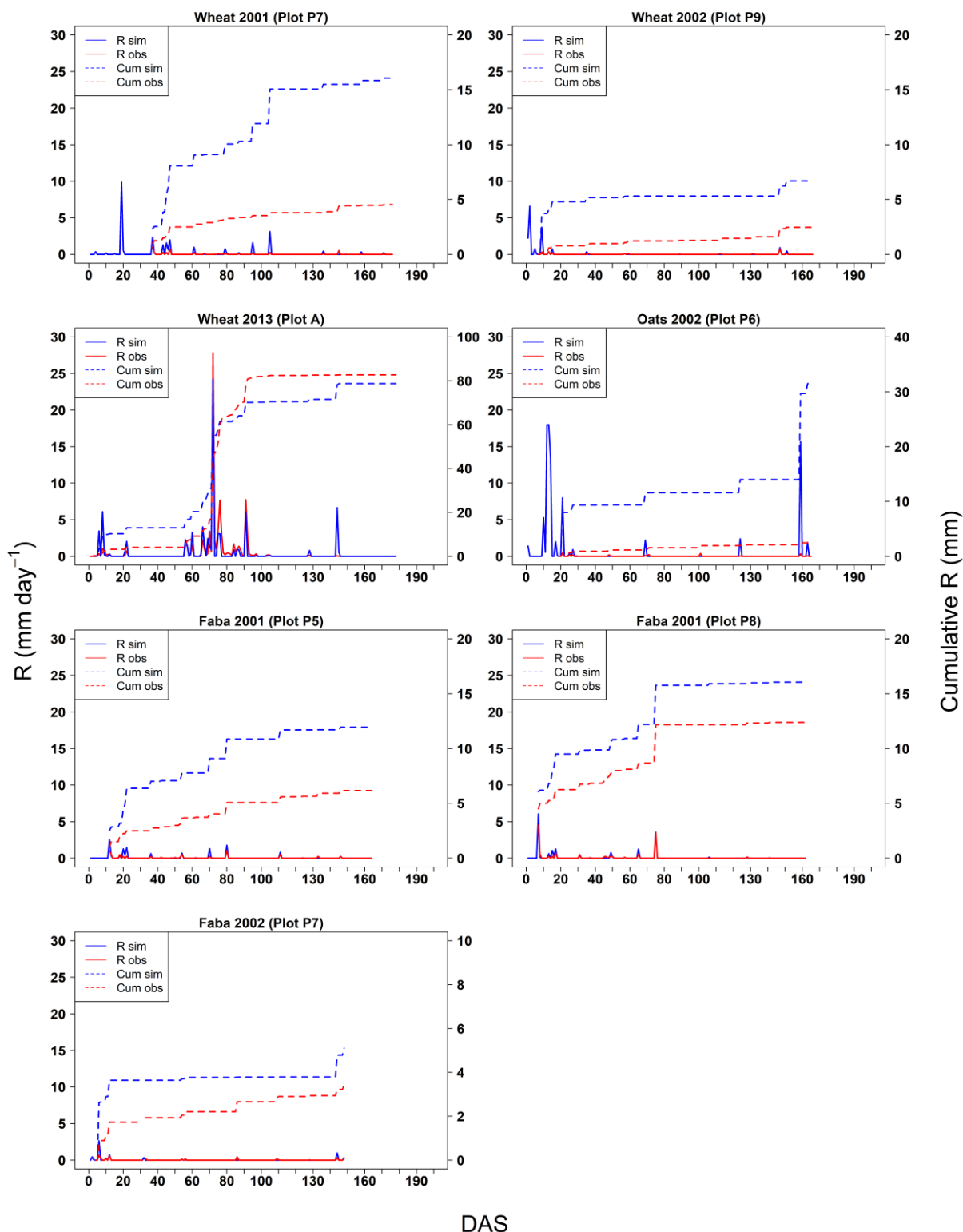
116



117

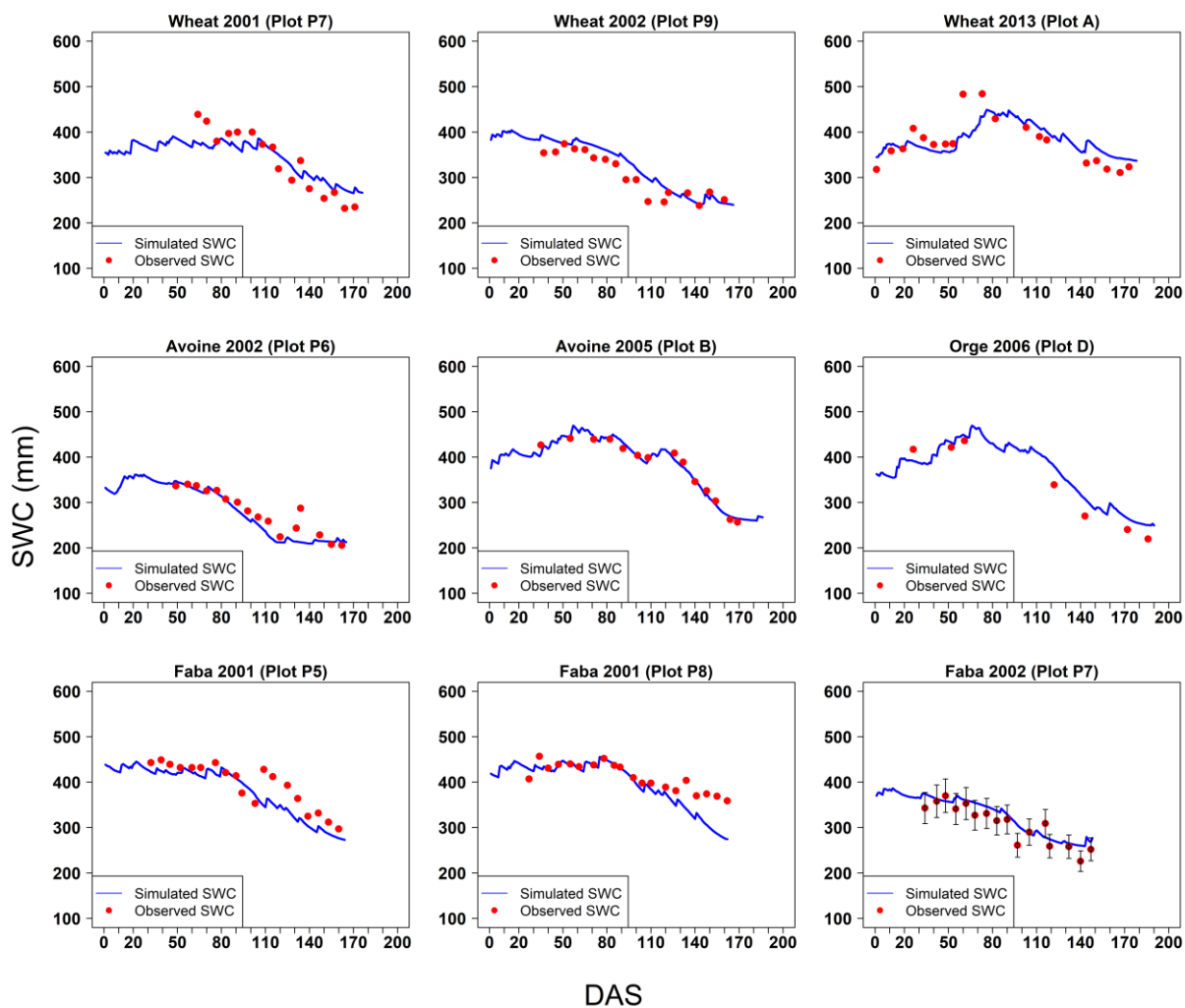
118 **Fig. SP4.** Temporal evolution of actual evapotranspiration (ETa) for each dataset when
119 available. The red curve corresponds to ETa simulated by AquaCrop, the green curve
120 corresponds to ETa measured in-situ by eddy covariance and the blue curve corresponds to
121 reference evapotranspiration ET0. DAS stands for Day after Sowing.

122



124

125 **Fig. SP5.** Temporal evolution of runoff (R) for each dataset when available. The solid lines
 126 represent the temporal evolution of R. The dashed lines represent R accumulation. The blue
 127 colour indicates the simulations and the red colour indicates the observations. DAS stands for
 128 Day after Sowing. Y-Scales are chosen for both reading and intercomparing.



130
 131 **Fig. SP6.** Temporal evolution of soil water content (SWC) for each dataset. The red points
 132 correspond to SWC observations, and the blue curves correspond to the AquaCrop
 133 simulations. DAS stands for Day after Sowing.

134
 135

136 **References**

- 137 Abrha, B., Delbecque, N., Raes, D., Tsegay, A., Todorovic, M., Heng, L., Vanutrecht, E.,
138 Geerts, S., Garcia-Vila, M., Deckers, S., 2012. Sowing strategies for barley
139 (HORDEUM VULGARE L.) based on modelled yield response to water with
140 AQUACROP. *Experimental Agriculture* 48, 252–271.
- 141 Araya, A., Habtu, S., Hadgu, K.M., Kebede, A., Dejene, T., 2010. Test of AquaCrop model in
142 simulating biomass and yield of water deficient and irrigated barley (*Hordeum vulgare*).
143 *Agricultural Water Management* 97, 1838–1846.
- 144 Belhouchette, H., Breaudeau, E., Hachicha, M., Donatelli, M., Mohtar, R.H., Wery, J., 2008.
145 Integrating spatial soil organization data with a regional agricultural management
146 simulation model: a case study in Northern Tunisia. *Transactions of the ASABE* 51,
147 1099–1109.
- 148 Cassel, D.K., Nielsen, D.R., 1986. Field Capacity and Available Water Capacity, in: Klute, A.
149 (Ed.), *SSSA Book Series*. Soil Science Society of America, American Society of
150 Agronomy, Madison, WI, USA, pp. 901–926.
- 151 Demarez, V., Duthoit, S., Baret, F., Weiss, M., Dedieu, G., 2008. Estimation of leaf area and
152 clumping indexes of crops with hemispherical photographs. *Agricultural and Forest*
153 *Meteorology* 148, 644–655.
- 154 Fang, H., Ye, Y., Liu, W., Wei, S., Ma, L., 2018. Continuous estimation of canopy leaf area
155 index (LAI) and clumping index over broadleaf crop fields: An investigation of the
156 PASTIS-57 instrument and smartphone applications. *Agricultural and Forest*
157 *Meteorology* 253–254, 48–61.
- 158 Jeuffroy, M.-H., Ney, B., 1997. Crop physiology and productivity. *Field Crops Research*,
159 *Improvement of Grain Legumes* 53, 3–16.
- 160 Jin, X., Feng, H., Zhu, X., Li, Z., Song, S., Song, X., Yang, G., Xu, X., Guo, W., 2014.
161 Assessment of the AquaCrop Model for Use in Simulation of Irrigated Winter Wheat
162 Canopy Cover, Biomass, and Grain Yield in the North China Plain. *PLOS ONE* 9,
163 e86938.
- 164 Pereira, L.S., Paredes, P., Rodrigues, G.C., Neves, M., 2015. Modeling malt barley water use
165 and evapotranspiration partitioning in two contrasting rainfall years. *Assessing*
166 *AquaCrop and SIMDualKc models*. *Agricultural Water Management* 159, 239–254.

- 167 Revaillot, S., Pouget, C., Alvarez, G., Fontaine, S., 2021. Mesurer la capacité de rétention en
168 eau d'un sol par centrifugation : une méthode fiable, facile et rapide à mettre en œuvre
169 dans un laboratoire (Les Cahiers des techniques de l'INRA). INRA.
- 170 Saxton, K.E., Rawls, W.J., 2006. Soil Water Characteristic Estimates by Texture and Organic
171 Matter for Hydrologic Solutions. *Soil Science Society of America Journal* 70, 1569–
172 1578.
- 173 Sreelash, K., Buis, S., Sekhar, M., Ruiz, L., Kumar Tomer, S., Guérif, M., 2017. Estimation of
174 available water capacity components of two-layered soils using crop model inversion:
175 Effect of crop type and water regime. *Journal of Hydrology* 546, 166–178.
- 176 Weiss, M., Baret, F., de Solan, B., Demarez, V., Bertrand, N., 2008. CAN-EYE, logiciel de
177 traitement d'images pour l'estimation de l'indice foliaire. *Le cahier des techniques de*
178 *l'INRA. Pratique et outils de mesure des rayonnements naturels* 159–166.
- 179 Yuan, M., Zhang, L., Gou, F., Su, Z., Spiertz, J.H.J., van der Werf, W., 2013. Assessment of
180 crop growth and water productivity for five C3 species in semi-arid Inner Mongolia.
181 *Agricultural Water Management* 122, 28–38.
- 182 Zeleke, K.T., 2019. AquaCrop Calibration and Validation for Faba Bean (*Vicia faba* L.) under
183 Different Agronomic Managements. *Agronomy* 9, 320.